

Effect of Physical Parameterization Schemes on Track and Intensity of Cyclone LAILA Using WRF Model

Radhika D. Kanase and P. S. Salvekar

Indian Institute of Tropical Meteorology, Pune, India

(Manuscript received 26 July 2014; accepted 22 June 2015)

© The Korean Meteorological Society and Springer 2015

Abstract: The objective of the present study is to investigate in detail the sensitivity of cumulus parameterization (CP), planetary boundary layer (PBL) parameterization, microphysics parameterization (MP) on the numerical simulation of severe cyclone LAILA over Bay of Bengal using Weather Research & Forecasting (WRF) model. The initial and boundary conditions are supplied from GFS data of $1^\circ \times 1^\circ$ resolution and the model is integrated in three 'two-way' interactive nested domains at resolutions of 60 km, 20 km and 6.6 km. Total three sets of experiments are performed. First set of experiments include sensitivity of Cumulus Parameterization (CP) schemes, while second and third set of experiments is carried out to check the sensitivity of different PBL and Microphysics Parameterization (MP) schemes. The fourth set contains initial condition sensitivity experiments. For first three sets of experiments, 0000 UTC 17 May 2010 is used as initial condition. In CP sensitivity experiments, the track and intensity is well simulated by Betts-Miller-Janjic (BMJ) schemes. The track and intensity of LAILA is very sensitive to the representation of large scale environmental flow in CP scheme as well as to the initial vertical wind shear values. The intensity of the cyclone is well simulated by YSU scheme and it depends upon the mixing treatment in and above PBL. Concentration of frozen hydrometeors, such as graupel in WSM6 MP scheme and latent heat released during auto conversion of hydrometeors may be responsible for storm intensity. An additional set of experiments with different initial vortex intensity shows that, small differences in the initial wind fields have profound impact on both track and intensity of the cyclone. The representation of the mid-tropospheric heating in WSM6 is mainly controlled by amount of graupel hydrometeor and thus might be one of the possible causes in modulating the storm's intensity.

Key words: Tropical cyclone, WRF model, physical parameterization, initial conditions

1. Introduction

Tropical cyclones that form over the Bay of Bengal during pre and post monsoon seasons cause considerable damage and destruction to lives and property over the east coast of India & Bangladesh. The destruction is due to strong gale winds, torrential rain and associated tidal wave. Timely and reasonably accurate prediction of the tracks and intensities of such

cyclones can minimize the loss of human lives and damage to properties. Though the general movement of the tropical cyclones is well known, it is desirable to have as much as accurate landfall prediction as possible for effective implementation of the disaster mitigation. There have been considerable improvements in the development of numerical models with increasing computer resources during recent decade. However application of numerical models for tropical cyclone prediction necessitates a study of suitable physics. Tropical cyclones originate over the ocean, where conventional meteorological observations tend to be sparse on a daily routine basis. Due to lack of data, deficiencies in model initial conditions lead to inaccurate forecasts of tropical cyclones (Lorenz, 1963; Mullen, 1989; Pielke, 2006). Knowledge of the physical processes that control tropical cyclone evolution is also limited. Thus, the forecasting of tropical cyclone track and intensity remains a challenging problem to the modeling community. As suggested by White et al. (1999) and Cacciamani et al. (2000) insufficient model resolution, inadequate physical parameterization, lack of sufficient detail or accuracy in the initial and boundary conditions (IBCs) or any combination of three may be the possible reasons for the poor forecast.

In the literature, it is found that the chief physical process for the intensification of low pressure into cyclonic storm is known to be the conditional instability of second kind (CISK) i.e., the cooperative interaction between the cloud scale and synoptic scale circulations (Chamey and Eliassen, 1964). Emanuel et al. (1994) noticed that CISK theory completely overlooks the role of surface moisture fluxes in accomplishing the re-moistening and thus the cyclone intensification in CISK would be just as likely to occur over land as over the sea, which is contradictory to observations. Another concern in CISK theory is coined by Smith (1997) about the heating representation which is simply a representation of moist pseudo-adiabatic ascent and is not a true sub-grid scale parameterization of deep convection in usual sense. The principal theory proposed as an alternative to CISK and cooperative intensification theory was introduced by Emanuel (1986) as air-sea interaction instability which is more recently named as Wind Induced Surface Heat Exchange (WISHE, Emanuel et al., 1994). In this theory the atmosphere is assumed to be neutrally stratified along the sloping surfaces of constant angular momentum. Moist convection mixes the air through

Corresponding Author: Radhika D. Kanase, Indian Institute of Tropical Meteorology, Pashan Rd, Panchawati, Pashan, Pune, Maharashtra 411008, India.
E-mail : radhikakanase@gmail.com

the troposphere but does not cause any temperature perturbations unless the boundary layer is heated by surface fluxes of heat and moisture. The surface fluxes are wind speed dependent and thus determined by the vortex-scale flow. Again a positive feedback cause a more intense cyclones producing more rapid heating of the atmosphere organized in such a way to intensify the cyclone which results in an instability. In very recent paper by Montgomery et al. (2015), different aspects of WISHE by different researchers are explained in detail Montgomery et al. (2009) and Montgomery et al. (2015) refute that the WISHE mechanism is the essential and dominant mode of tropical cyclone intensification in the prototype problem. All the mechanism of cyclone intensification is explained in detail in Montgomery and Smith (2011). Thus the exchange of energy at the ocean-atmosphere interface and its supply through the planetary boundary layer to the free atmosphere play an important role in the development of tropical storms and hence need to be carefully represented in the numerical models for realistic predictions (Anthes, 1982; Ross and Kurihara, 1995).

A number of cumulus parameterization schemes (CPS) have been developed and their role with PBL and microphysics parameterization (MP) in the simulation of tropical cyclone (TC) using different mesoscale models are also studied by many researchers. Hill and Lackmann (2009) studied the sensitivity to PBL parameterization (MYJ and YSU) and horizontal grid spacing (36-, 12-, 4-km) for a wide variety of idealized vortices, ranging from an unbalanced warm bubble to fully balanced vortices with KF as CPS & Lin schemes as MPS for all the experiments. They found that YSU scheme with horizontal grid spacing of 4 km incorporates values of exchange coefficient for moisture more consistently with the observations and leads to simulated TC intensity comparable to empirical estimates of maximum intensity. Couple of studies mentioned above used WRF model. Bhaskar Rao et al. (2006, 2007) and Srinivas et al. (2007) examined the role of CPS, PBL and MPS on track & intensity of tropical cyclone using MM5. These studies indicate that convective processes control the movement of the model storm while PBL processes are crucial in determining the intensity of cyclone. Some of the studies (Li and Pu, 2008; Mukhopadhyay et al., 2011; Tao et al., 2011; Efstathiou et al., 2012) suggested the combination WSM6-YSU as MP and PBL schemes works better for different weather systems. Srinivas and Bhaskar Rao (2014) studied the sensitivity for Orissa Super cyclone and found that Kain-Fritsch, MYJ (Efstathiou et al., 2013) and Lin cloud microphysics has performed better for the track and intensity simulation. Raju et al. (2011) reported slightly higher better track errors of NARGIS as 136, 252 and 381 km at 24, 48 and 72 hrs respectively with MYJ PBL scheme. Very recent study by Hariprasad et al. (2014) examined the sensitivity of different PBL schemes at Kalpakkam (a tropical site) and demonstrated that YSU scheme simulated various PBL quantities are in better agreement with the observations. Thus, there are different opinions of PBL schemes as well as MP schemes

for different intense events. Therefore, MYJ and YSU as PBL schemes and Ferrier and WSM6 as MP schemes are not yet tested for relatively weak intensity cyclones over NIO.

Several simulation studies have been conducted to understand the TCs over the NIO using high resolution mesoscale models (Trivedi et al., 2006; Li and Pu, 2008; Pattanayak and Mohanty, 2008; Bhaskar Rao et al., 2009; Deshpande et al., 2010, 2012; Srinivas et al., 2010; Mukhopadhyay et al., 2011; Raju et al., 2011; Tao et al., 2011; Efstathiou et al., 2012; Osuri et al., 2012, 2013). These studies are based on evaluating the model performance with respect to physics sensitivity, resolution, initial conditions and impact of data assimilation on the track and intensity forecast of very severe cyclones. However, there is another class of TC which does not reach the stage of very severe cyclonic storm but attains lesser intensity, named as weak cyclones. These weak cyclones (Severe Cyclonic Storms and Cyclonic Storms), due to their slow motion and quasi-stationary nature cause very heavy rainfall and in turn large amount of damage to the property. Very few studies have focused on simulating the weak intensity storms (Osuri et al., 2013; Srinivas et al., 2013), but the detailed evolutions behind the success or failure of physical parameterization is hardly addressed. Thus one of the objectives of the present study is to find out the reason behind the better performance of physical parameterization scheme in simulating weak cyclones. Kanase and Salvekar (2014a), Yesubabu et al. (2014) have worked on the numerical study of cyclone LAILA by studying its vertical structure as well as role of nudging factor respectively. Srinivas et al. (2013) studied the sensitivity of 21 cyclones including cyclone LAILA but detailed reason behind the success/failure in simulating the different cyclones by different physical parameterization schemes is not yet reported.

In mesoscale models, large scale global analyses provide the initial condition to the mesoscale models. So the initial conditions may not be able to capture the intensity and location of the initial vortex to give correct forecast of TCs. Importance of accurate initial conditions is studied by Arpe et al. (1985), Sanders (1987), Kuo and Reed (1988), Mohanty et al. (2010). NWP being an initial value problem, Lorenz (1963) and Pielke (2006) have shown that even a small error in the initial condition (IC) may lead to a large error in the subsequent forecast. Effect of initial condition from different data sources on the numerical simulation of Orissa Super Cyclone is studied by Trivedi et al. (2002) by generating the synthetic vortex data using empirical relation. Pattanaik and Rama Rao (2009) studied the case of very severe cyclone 'Nargis' with four different initial conditions (28th April, 29th April, 30th April and 1st May) after the formation of depression with the combination of YSU as PBL, Grell-Devenyi as CPS and WSM 3 simple ice as MPS using WRF model. They concluded that 30th April and 1st May initial conditions gives less landfall errors of 85 km and 50 km. Mohanty et al. (2010) explored the impact of different sources of initial and boundary conditions on track and intensity of the Bay of Bengal

cyclones.

For a numerical modeler, it is required to know the intensity of the initial vortex that can give better prediction of TCs. To our knowledge, there is hardly any work available in the literature to examine the role of initial condition starting from different initial states of the system [i.e., prior to formation of low pressure area (LoPar), LoPar and prior to formation of Depression (D)]. Basically these initial conditions are very useful for timely warning as well as effective implementation of disaster mitigation. Thus the main objective of the present study are to evaluate the influence of the choice of physical parameterization and also to study the impact of initial conditions (started from different intensity of the initial vortices) on simulating track and intensity of the weak cyclone. We also tried to find out the physical and dynamical reasons behind the success/failure of physical parameterization scheme and initial condition.

The paper is arranged in five sections. After introduction, a brief description of model and experimental design are described in section 2, followed by brief description of cyclone in section 3. The results are discussed in section 4 and conclusions of the study are presented in section 5.

2. Model description and experimental design

a. WRF model

The Advanced Research Weather Research and Forecasting (WRF-ARW) version 3.2 mesoscale model developed by National Center for Atmospheric Research (NCAR) is used in the present study. The model incorporates fully incompressible

non-hydrostatic equations and uses a terrain following vertical coordinate. The model is versatile with a number of options for nesting, boundary conditions, data assimilation and parameterization schemes for subgrid-scale physical processes (Skamarock et al., 2008). The details of the experiments performed are given in Table 1.

The convection schemes compute vertical fluxes due to updrafts and downdrafts and compensating motion outside the clouds. Four convective parameterization schemes (CPS) such as Kain-Fritsch (KF), Betts-Miller-Janjic (BMJ), Grell-Devenyi (GD) and Grell are used in the present study. The KF scheme follows a Lagrangian parcel method and uses a simple cloud model with moist updrafts and downdrafts, including the effects of detrainment and entrainment (Kain, 2004). It has a trigger function, a mass flux formulation and a closure based on the removal of convective available potential energy (CAPE) in a grid column. Its activation at a particular grid is decided by trigger function which is based on the vertical motion. The BMJ scheme is a convective adjustment scheme and it depends on a non-dimensional parameter called 'cloud efficiency' which is a function of mean temperature of cloud, entropy change and precipitation (Betts and Miller, 1986; Janjic, 2000). The scheme essentially removes the conditional instability in each grid column by adjusting the vertical profile of temperature and specific humidity toward the reference profile (Betts, 1986; Betts and Miller, 1986). This scheme does not include the moist processes below the cloud base as well as in the lower boundary layer. The scheme gets triggered if a parcel which is lifted moist adiabatically from the lower troposphere to a level above the cloud base becomes warmer than the environment. The Grell-Devenyi (GD) is a cloud

Table 1. Overview of WRF model configuration for the experiments of physical parameterization sensitivity and Initial condition sensitivity.

Model Used	WRFV3.2.1
Initial and boundary conditions	GFS data of $1^\circ \times 1^\circ$ resolution
Domains with horizontal and vertical Resolution	D1 (60 km), D2 (20 km) and D3 (6.6 km) with 28 vertical levels
No. of horizontal grid points in X-Y direction	D1- 52×52 ; D2- 121×121 ; D3- 211×271
Period of integration	For physical parameterization sensitivity: D1: 0000 UTC 17 May 2010 D2: 0600 UTC 17 May 2010 D3: 1200 UTC 17 May 2010 For initial condition sensitivity experiments: outermost domain (D1) starts from 0000 UTC 15 May 2010, 0000 UTC 16 May 2010 and 0000 UTC 17 May 2010. Rest of the domains start at the same time as that of the physical parameterizations sensitivity experiments. For all the experiments, model is integrated till 0600 UTC 21 May 2010.
Cumulus parameterization schemes (CPS)	BMJ, KF, GD and Grell
PBL parameterization schemes (PBL)	MYJ and YSU
Microphysics parameterization schemes (MPS)	Ferrier and WSM6
Radiation parameterization scheme	Short wave: RRTM Long wave: Dudhia
Surface layer scheme	Monin-Obukhov scheme
Land-surface scheme	Unified Noah land-surface model

ensemble scheme. The unique aspect of the GD scheme is that it uses 16 ensemble members derived from 5 popular closure assumptions to obtain an ensemble mean realization at a given time and location. The details for obtaining mean are provided by Grell and Devenyi (2002). Grell-3 scheme (hereafter referred as Grell in the text) allows the subsidence effect to be spread to neighboring grid columns, which makes it more suitable to grid sizes less than 10 km. But this scheme can also be used at larger grid sizes where subsidence occurs within the same column as the updraft.

Two bulk microphysical parameterization schemes (MP), Eta Ferrier (hereafter referred as Ferrier in the text) and WSM6 are considered. Ferrier is the new cloud and precipitation scheme used in the operational Eta model over United States of America (USA) introduced in 2001. Ferrier predicts total condensate, which is the sum of cloud water, rain water and cloud ice. All these condensate can co-exist at temperatures warmer than -10°C . The ice category in Ferrier includes small ice crystals mainly dominant in the cirrus and upper tropospheric clouds, and larger ice particles in the form of snow, graupel and sleet which are dominant at lower levels. Details about Ferrier can be found at <http://www.emc.ncep.noaa.gov/mmb/mmbp11/eta12tpb>. In WRF Single-Moment 6-class (WSM6) Microphysics scheme, '6' stands for six classes of hydrometeors including graupel. Dudhia et al. (2008) modified Hong and Lim (2006) mixed-phase microphysics scheme to allow for a more realistic representation of partially rimed particles. The new scheme assigns a single fall speed to snow and graupel which is weighted by mixing ratio and this fall speed is applied to both sedimentation and accretion processes.

Yonsei University and Mellor-Yamada-Janjic PBL parameterization schemes are used in the present study. The Yonsei University Planetary Boundary Layer (YSU PBL) scheme (Hong et al., 2006) is modified MRF PBL (Hong and Pan, 1996) scheme with an explicit treatment of the entrainment layer at the PBL top. It uses the counter-gradient terms to represent fluxes due to non-local gradients and smaller magnitude of the counter-gradient mixing in the YSU PBL produces a well-mixed boundary layer profile. Mellor-Yamada-

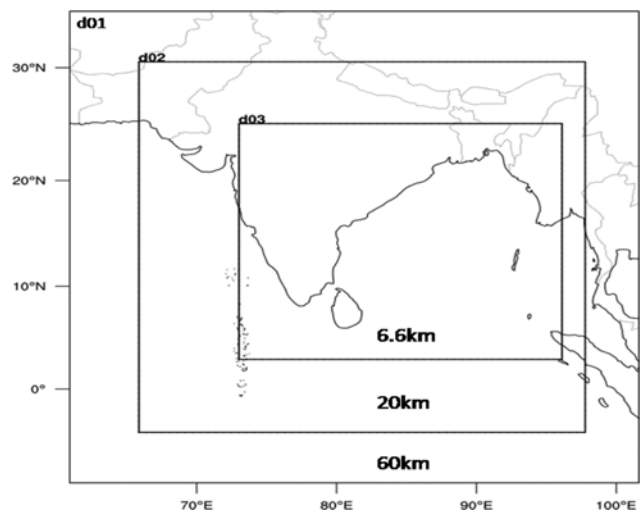


Fig. 1. Model Domains with d01-60 km, d02-20 km, and d03-6.6 km for cyclone LAILA.

Janjic (MYJ) parameterization of turbulence in boundary layer and in the free atmosphere (Janjic, 1990, 1996, 2002) represents a non-singular implementation of Mellor-Yamada Level 2.5 turbulence closure model (Mellor and Yamada, 1982) through the full range of atmospheric turbulent regimes. In this implementation, an upper limit is imposed on the master length scale. This upper limit depends on Turbulent Kinetic Energy (TKE) and buoyancy as well as shear of the driving flow. More details can be found in Janjic (1996, 2002).

For long wave radiation parameterization, Rapid Radiative Transfer Model (RRTM) scheme on Mlawer et al. (1997) and for short wave Dudhia scheme based on Dudhia (1989) are used.

b. Experimental design and data

Total four sets of experiments are carried out in the present study using WRF model. First three sets of experiments deals with the different physical parameterization schemes such as

Table 2. Different sensitivity experiments carried out in the study.

	Experiment	Cumulus	Microphysics	PBL	Initial Condition (IC)	
Physical Parameterization Sensitivity	CPS sensitivity	BMJ	WSM6	YSU	0000 UTC 17 May 2010	
		KF	WSM6	YSU	0000 UTC 17 May 2010	
		GD	WSM6	YSU	0000 UTC 17 May 2010	
		Grell	WSM6	YSU	0000 UTC 17 May 2010	
	MPS sensitivity	BMJ*	WSM6	YSU	0000 UTC 17 May 2010	
			Ferrier	YSU	0000 UTC 17 May 2010	
		PBL sensitivity	BMJ*	WSM6	YSU	0000 UTC 17 May 2010
			BMJ	WSM6	MYJ	0000 UTC 17 May 2010
IC Sensitivity	15 May	BMJ	WSM6	YSU	0000 UTC 15 May 2010	
	16 May	BMJ	WSM6	YSU	0000 UTC 16 May 2010	
	17 May	BMJ*	WSM6	YSU	0000 UTC 17 May 2010	

* Same experiment as in CPS sensitivity with BMJ scheme

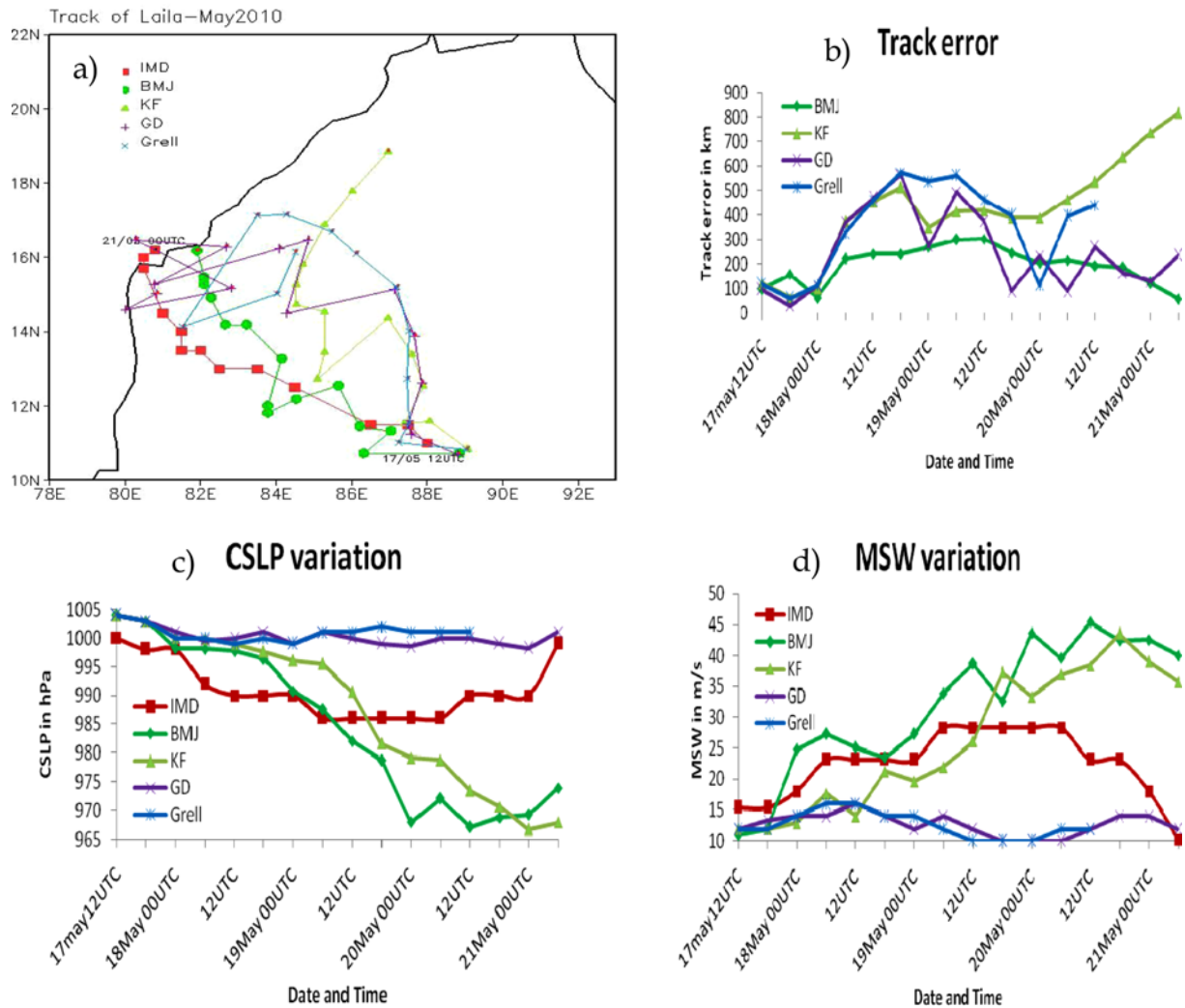


Fig. 2. a) Model simulated tracks, b) time evolution of track error, c) time series plot of minimum central sea level pressure (CSLP) in ha and d) time series of maximum surface wind speed (MSW) for different experiments with different cumulus parameterization (CP) schemes along with IMD best fit track, CSLP and MSW data. The time interval of track and intensity is 6 hrs.

CP, PBL and MP. The model is integrated beyond 12 hrs of observed landfall with three two-way nested domains having horizontal resolution of 60 km, 20 km and 6.6 km (Fig. 1). The initial and lateral boundary conditions are supplied from Global Forecast System (GFS) data of $1^\circ \times 1^\circ$ resolutions and for physical parameterization sensitivity experiments model integration is started from 0000 UTC 17 May 2010. The model configuration used in the present study is summarized in Table 1. For CP sensitivity, BMJ, KF, GD and Grell schemes are checked by keeping YSU as PBL and WSM6 as MP schemes fixed. The second set of PBL parameterization scheme included sensitivity of YSU and MYJ schemes with BMJ and WSM6 kept fixed. Ferrier and WSM6 are the two schemes which are tested in MP sensitivity experiments with rest of the configuration kept same. To demonstrate the impact of different initial conditions starting from different initial vortex intensity, fourth (an additional) set of experiments is carried

out with three different initial vortex intensity i.e., initial conditions starting from different analysis time such as 0000 UTC 15 May 2010 (15 May), 0000 UTC 16 May 2010 (16 May) and 0000 UTC 17 May 2010 (17 May). These different initial conditions show small differences in the wind fields e.g., 15 May: 24 hrs prior to formation of Low Pressure Area (LoPar), 16 May: LoPar and 17 May: 6 hrs prior to Depression. The combination BMJ-YSU-WSM6 as CP-PBL-MP schemes is same for the last group of experiments. The details of the sensitivity experiments carried out are summarized in Table 2.

3. Description of cyclone LAILA

The cyclone ‘LAILA’ which formed during May 2010 is the first pre-monsoon severe cyclone that crossed Andhra Pradesh coast after 1990. Under the influence of onset of southwest

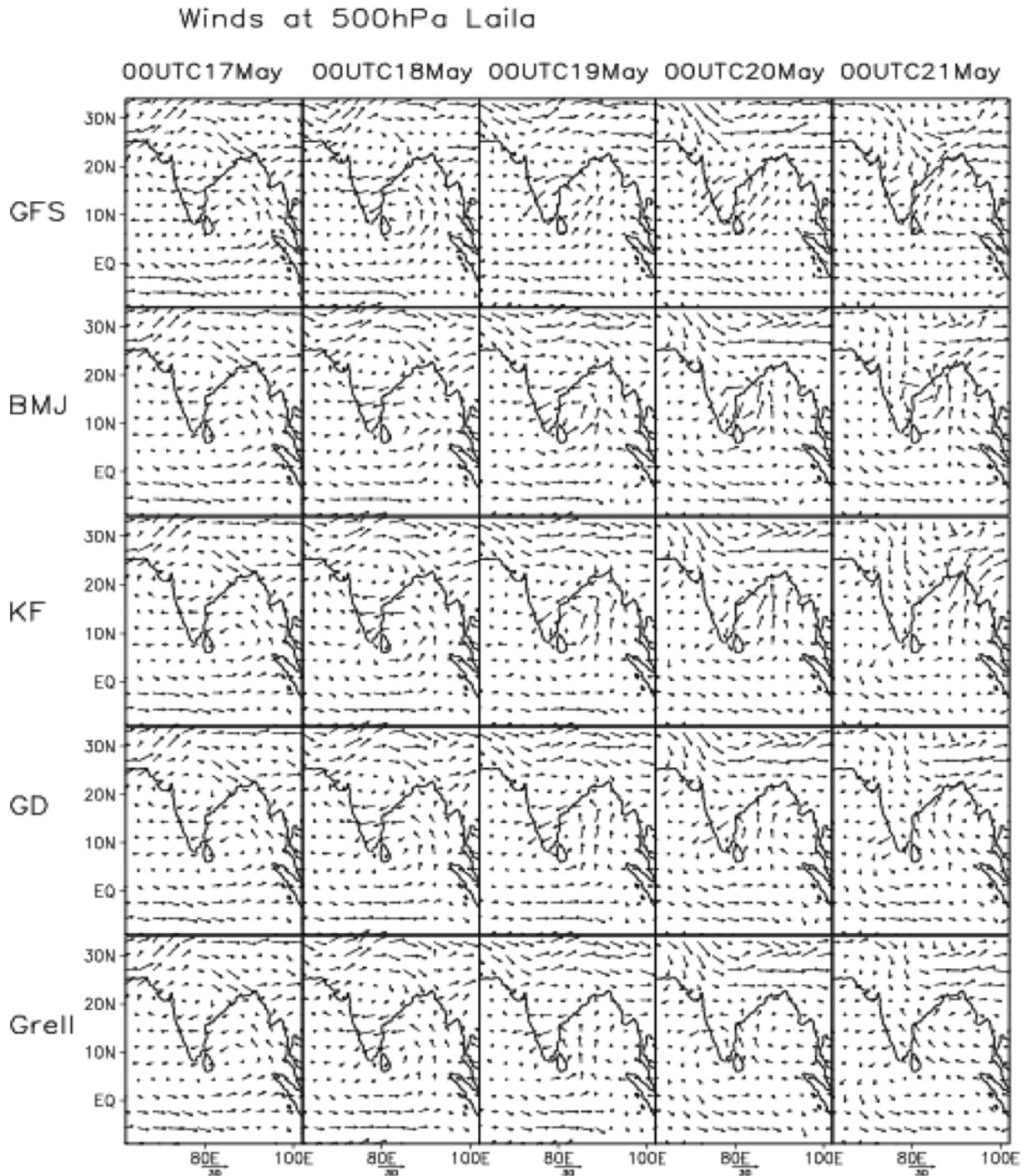


Fig. 3. Wind fields at 500 hPa level for CP experiments in the outermost domain (D1 60 km), starting from the initial condition at 0000 UTC 17 May with every 24 hrs of interval.

monsoon over Andaman Sea and adjoining south BoB, the low level circulation turned to be a low pressure area on 1200 UTC 16 May with center near $9.0^{\circ}\text{N}/90.5^{\circ}\text{E}$. It concentrated into depression on 0600 UTC 17 May and further into deep depression on 1200 UTC 17 May over southeast BoB, about 850 km east-southeast of Chennai. It moved westward and intensified into cyclonic storm at 0000 UTC 18 May, near

$11.5^{\circ}\text{N}/86.5^{\circ}\text{E}$ with Central Sea Level Pressure (CSLP) of 998 hPa and Maximum Surface Wind speed (MSW) of 18 m s^{-1} . The cyclone further intensified into severe storm on 0600 UTC 19 May and attained its maximum intensity of CSLP 986 hPa and MSW 29 m s^{-1} up to 0900 UTC 20 May. Cyclone moved slowly during landfall at Andhra Pradesh coast near Bapatla between 1100 and 1200 UTC 20 May 2010. It caused heavy

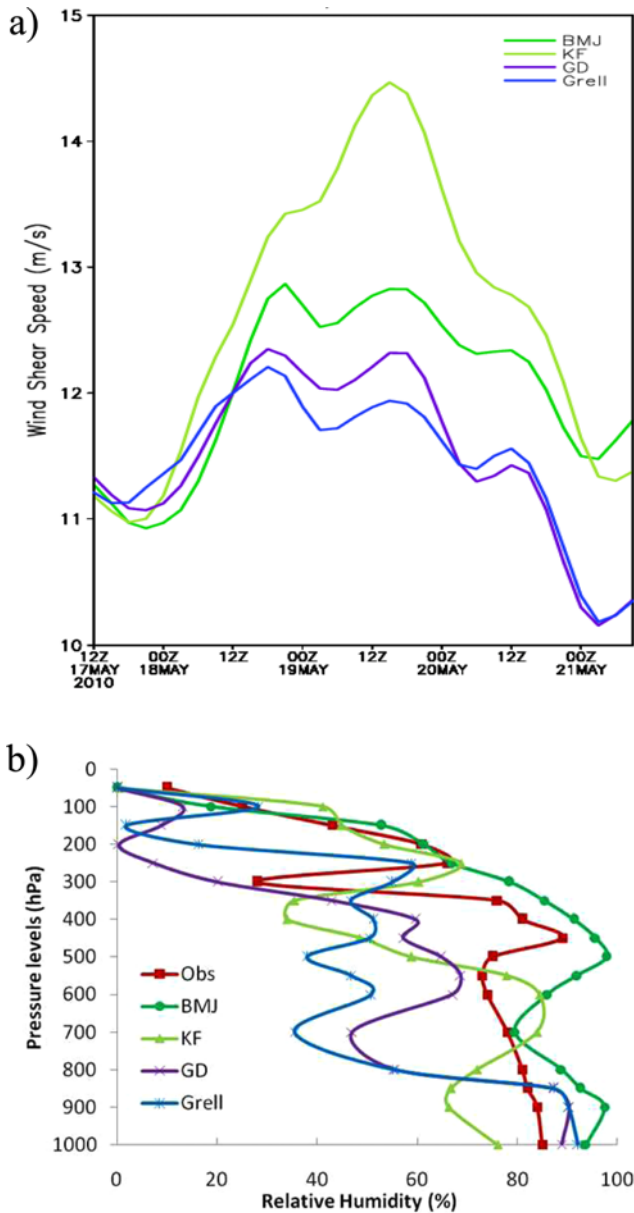


Fig. 4. a) Time series of wind shear speed (m s^{-1}) averaged over the outer domain for CP sensitivity experiments, b) Vertical profile of relative humidity at Machilipatnam Station near landfall i.e., at 0000 UTC 22 May 2010 for CP sensitivity experiments.

rainfall over coastal Andhra Pradesh and Tamil Nadu and flooding and damage along its path. The significant feature of the system is that it lay very close to the coast after landfall maintaining cyclone intensity for about 12 hrs after landfall. More detailed description as well as the performance of different forecast model can be found in RSMC Report (2011).

4. Results and discussion

In this study, First three set of experiments (Table 2) are conducted to study the sensitivity of three kinds of physical parameterization schemes (i.e., cumulus, microphysics and

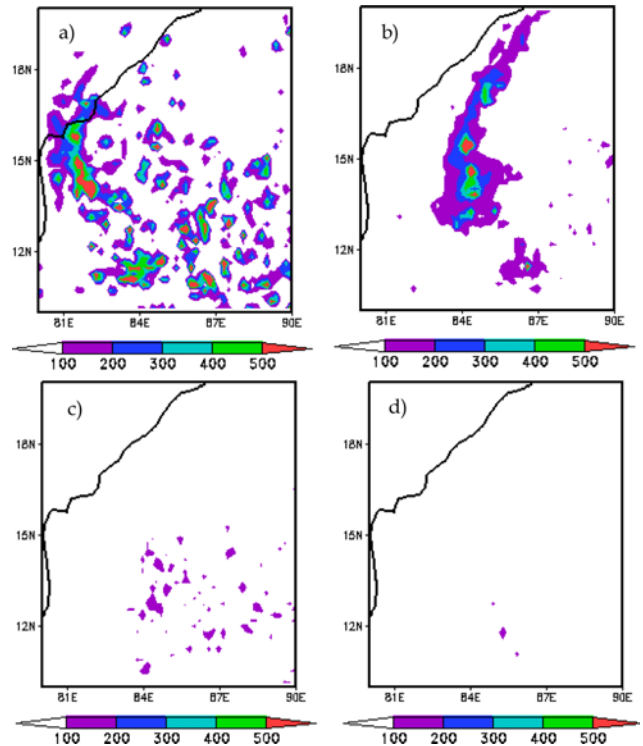


Fig. 5. Spatial distribution of middle level (500 hPa -300 hPa) heating (K Day^{-1}) for CPS experiment. a) BMJ, b) KF, c) GD, and d) Grell.

planetary boundary layer) and fourth set included the sensitivity of initial condition starting from different initial intensity of cyclone vortex (i.e., 0000 UTC 17 May, 0000 UTC 16 May and 0000 UTC 15 May 2010).

a. Sensitivity to cumulus parameterization schemes

In this group, four experiments are carried out with the variation only in the cumulus parameterization (CP) scheme. The CP schemes used are BMJ, KF, GD and Grell in combination with YSU as PBL scheme and WSM6 as MP scheme.

Figures 2a-d shows the model simulated tracks, time evolution of track error and intensity in terms of minimum CSLP and MSW along with observed best fit track and intensity obtained from India Meteorological Department (IMD) respectively for cyclone LAILA. The observed movement of the storm is in the North-west direction till the landfall of the storm. The track obtained (Fig. 2a) from BMJ experiment has captured the direction of movement of observed storm very well but with some eastward bias near landfall time whereas more eastward bias is observed in KF experiment. The track of GD and Grell experiments shows northward movement initially for first 2 days of integration and then north-westward movement with very irregular behavior. It is also observed from Fig. 2a that, the translational speed of the storm is little slower for BMJ and faster for KF, GD and Grell compared to observation. Throughout the integration period BMJ modeled storm moves closely to the

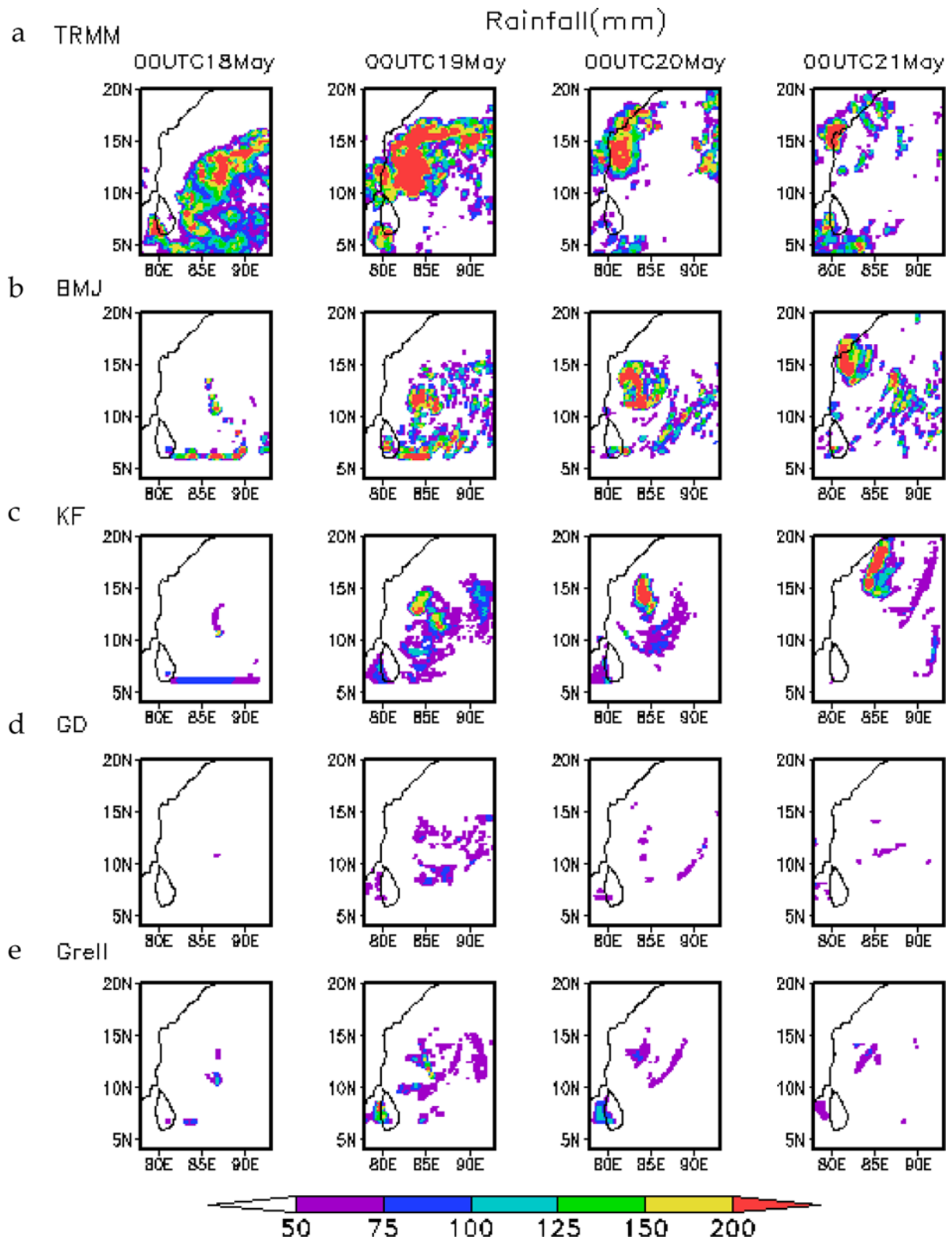


Fig. 6. 24 hrs accumulated rainfall (mm) at 0000 UTC 18 May, 0000 UTC 19 May, 0000 UTC 20 May and at 0000 UTC 21 May respectively, for a) TRMM, b) BMJ, c) KF, d) GD, and e) Grell.

observed track of the storm. The least track error (i.e., less than 250 km throughout integration time) is shown by BMJ ex-

periment, while track errors for KF increases with time. The intensity in terms of minimum CSLP and MSW is plotted in

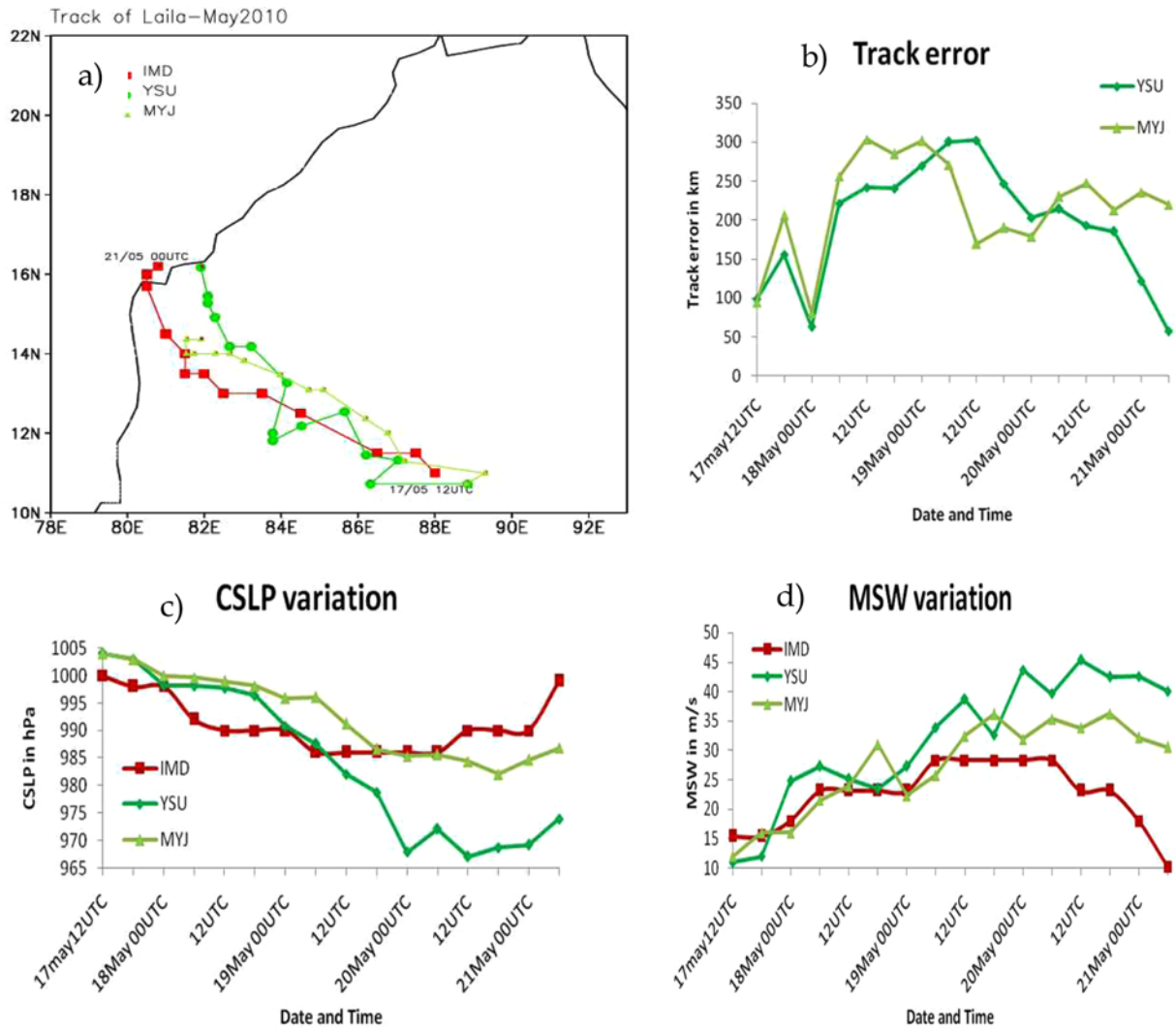


Fig. 7. a-d) Same as Fig. 2 but for the experiments with different planetary boundary layer (PBL) parameterization schemes.

Figs. 2c and d. The intensity is underestimated by GD and Grell (~1000 hPa) while it is overestimated by BMJ and KF (~967 hPa). For Grell experiment, the cyclonic circulation is dissipated much earlier and the cyclonic vortex did not reach the storm intensity for GD and Grell schemes (Figs. 2c, d). However considering track and intensity both in view, simulation from BMJ experiments are better in this group.

These results clearly explored the profound sensitivity of cyclone's track and intensity forecast to the variations in CP scheme. Now we will discuss some of the possible causes for these results. For this, the winds at 500 hPa level for each of these experiments in the outermost domain (60 km) and for GFS analysis data are plotted in Fig. 3. For BMJ and KF, up to 0000 UTC 19 May, the winds at 500 hPa level are in good agreement with the GFS observed upper level winds. After that, the cyclonic vortex at 500 hPa level in KF is shifted to the east side of the observed storm, whereas for BMJ the winds are still qualitatively matches with the GFS. The increased magnitude of northward winds to the east side of the cyclone

center and its interaction with the mid-latitude westerlies at 0000 UTC 20 May, may caused KF modeled storm to move away from the IMD observed track. For GD and Grell experiments, feeble cyclonic circulation is seen up to 0000 UTC 19 May and after that, no cyclonic circulation is observed at 500 hPa level. The weak westerlies in the lower tropospheric level i.e., at 850 hPa level (Figure not shown) and easterlies at the 500 hPa level may have produced strong wind shear which further prohibited the development and thus the intensification of the cyclonic storm LAILA in GD and Grell. Such easterlies are found to be absent in BMJ and KF at 500 hPa level which may have resulted into weak wind shear and thus more intense storm. Vertical wind shear of the environmental flow is considered an important factor that can limit both the intensification and intensity of a TC (Wu and Cheng, 1999; Emanuel, 2004; Wang and Wu, 2004). TCs are influenced by environmental wind shear at all stages of their life cycle (Gray, 1968; Tuleya and Kurihara, 1981; Merrill, 1988). Large shears produce a large ventilation of heat away from the

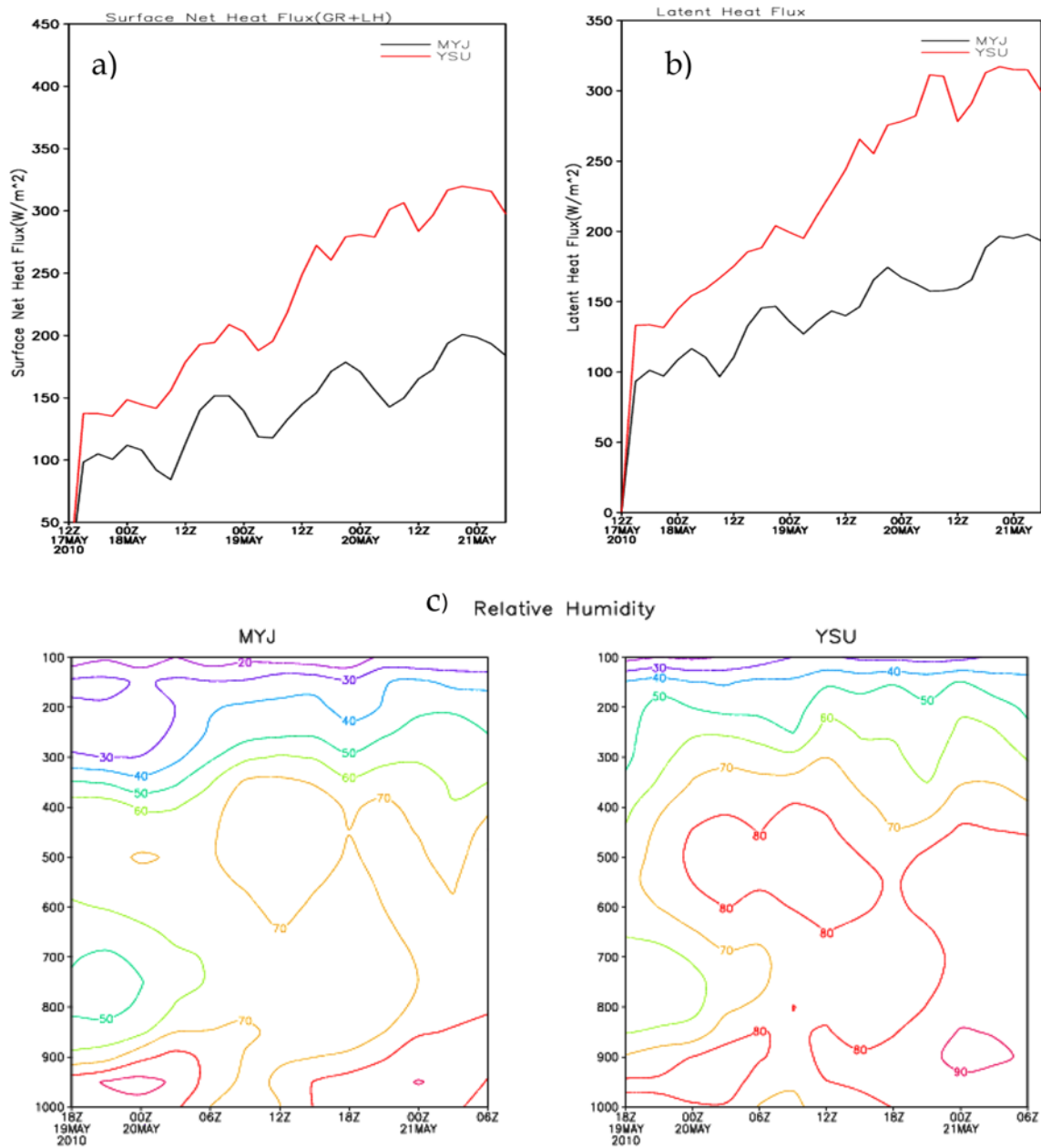


Fig. 8. Time series of a) surface net heat flux (SNHF) and b) latent heat flux in $W m^{-2}$ for PBL sensitivity experiments. c) Time evolution of relative humidity averaged over 5 degree around cyclone center and is plotted for maximum intensity period (i.e., 1800 UTC 19 May to 0600 UTC 21 May) for MYJ and YSU PBL schemes.

developing disturbance. Frank and Ritchie (2001), in their series of simulation experiments for testing impact of vertical wind shear, found that when relatively weak ($5 m s^{-1}$) shear is added to the mean flow, the simulated storms rapidly developed stronger. On the contrary, strong shear ($10-15 m s^{-1}$) dissipates the warm air in the upper layers, leading to overall weakening of the storm from the top to downward. The distribution of latent heat released depends upon the cumulus parameterization schemes. The condensation heat released by the cumulus cloud to the upper troposphere is advected in a different direction relative to the released heat at lower levels.

In an environment with strong shear, concentration of heat through the entire troposphere becomes more difficult, which inhibits the storm development (Gray, 1968). The cumulus parameterization scheme indirectly influences the wind shear. As we know, CPS schemes are largely controlled by large-scale environment; in addition, it also alters the large-scale environment through feedback mechanism.

To see the impact of CP schemes on the wind shear and thus on the intensification, time series of domain averaged, vertical wind shear (between 850 hPa and 200 hPa layers) of horizontal wind is plotted in Fig. 4a. There is a time lag between

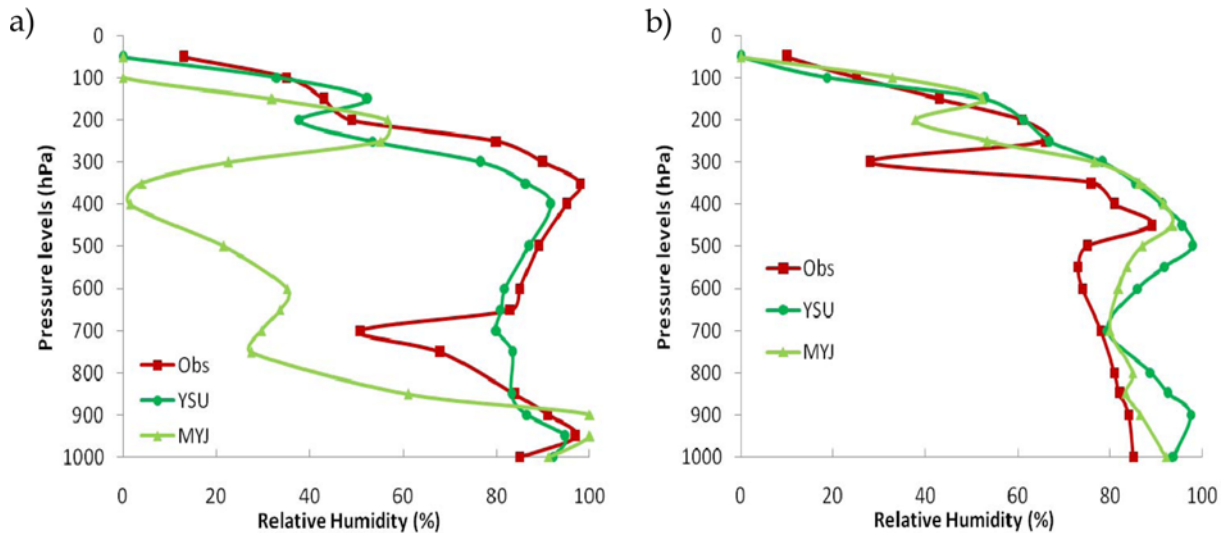


Fig. 9. Vertical profile of relative humidity at Machilipatnam station for PBL sensitivity experiments plotted at a) 0000 UTC 19 May 2010 and b) 0000 UTC 21 May 2010.

imposition of the shear and the resulting change in the minimum CSLP of simulated storms (Frank and Ritchie, 2001). Initial 12 hrs of integration (i.e., up to 0000 UTC 18 May 2010), the intensity is same for all the four schemes (Fig. 2), but shear is weak for BMJ ($\sim 11 \text{ m s}^{-1}$) and KF schemes (Fig. 4a) compared to GD and Grell simulated storms. The weak shear at the initial development stage of the storm might have helped the further development of the BMJ as well as KF simulated storm, whereas for GD and Grell simulated storms, high shear during initial 12 hrs of integration might have hampered further intensification. Observational studies also suggest that a TC cannot develop unless environmental vertical wind shear is below a certain threshold value i.e., $\sim 12.5 \text{ m s}^{-1}$ in Western North Pacific and $8\text{--}10 \text{ m s}^{-1}$ in Atlantic (Zehr, 1992; Ritchie, 2002). However evidence also shows that well-developed TCs can survive quite large vertical shear conditions (e.g., $15\text{--}20 \text{ m s}^{-1}$) over Western North Pacific (Zheng et al., 2007). Since BMJ and KF storm were well-developed, it could sustain and intensify further, though the shear is increasing from $\sim 11 \text{ m s}^{-1}$ to 14.5 m s^{-1} during 0000 UTC 18 May to 1200 UTC 19 May. Thereafter, decrease in the shear caused intensification of BMJ and KF simulated storm and attained its maximum intensity, up to 0000 UTC 21 May and then the BMJ simulated storm started dissipating (as it reached close to the land) whereas KF simulated storm still show higher intensity (as it is over ocean). To dig further the reason behind the intensification of storm by BMJ and KF, we have compared the relative humidity profiles from radiosonde observations (obtained from Wyoming University website) at Machilipatnam station (this is the only station close to cyclone) and those obtained from model simulated storms for all the CP schemes near landfall i.e., at 0000 UTC 21 May 2010 (Fig. 4b). BMJ simulated storm shows slightly higher values of relative humidity than the radiosonde observations,

especially the mid-tropospheric moisture profile is in close agreement with the observations. The mid-tropospheric relative humidity from BMJ is in close agreement with the observations whereas for other schemes it shows very dry surrounding. The KF simulated storms shows dry soundings which may be because of the storm moved away from the Machilipatnam station. GD and Grell simulated storms are also far away from the station, which may be one of the reason for showing dry surrounding. Thus, from Fig. 4b, it is clear that the humidity profile of BMJ is matching well the observations. The proper representation of mid-tropospheric heating gives the better intensity prediction of the storm (Mukhopadhyay et al., 2011). The spatial distribution of middle level (700 hPa–500 hPa) heating in K Day^{-1} is plotted in Fig. 5 for all the four CP schemes. The mid-tropospheric heating is found to be more in BMJ and KF which is may be due to the large amount of latent heat released during the autoconversion processes of hydrometeors within the core of cyclone. These processes may have slowed down in GD and Grell scheme which resulted into less heating in the mid-troposphere. Inner core rainfall is a good indicator of latent heat release, which is a crucial heat source for intensification and the rainfall intensity is significantly correlated with the intensity of the storms (Rodgers et al., 1994a, b). The simulated 24 hrs accumulated rainfall for every 24 hours i.e., at 0000 UTC 18 May, 0000 UTC 19 May, 0000 UTC 20 May and 0000 UTC 21 May 2010 for four CP schemes along with that obtained from Tropical Rainfall Measuring Mission (TRMM) data is plotted in Fig. 6. It can be seen that, the spatial area covered by the TRMM observations is reduced in BMJ and KF simulated storm during intensification period, but the magnitudes of the rainfall i.e., more than 200 mm by BMJ and KF, are well matching with the observations. The location of the rainfall maxima and the track of the cyclone simulated by BMJ and KF are in good

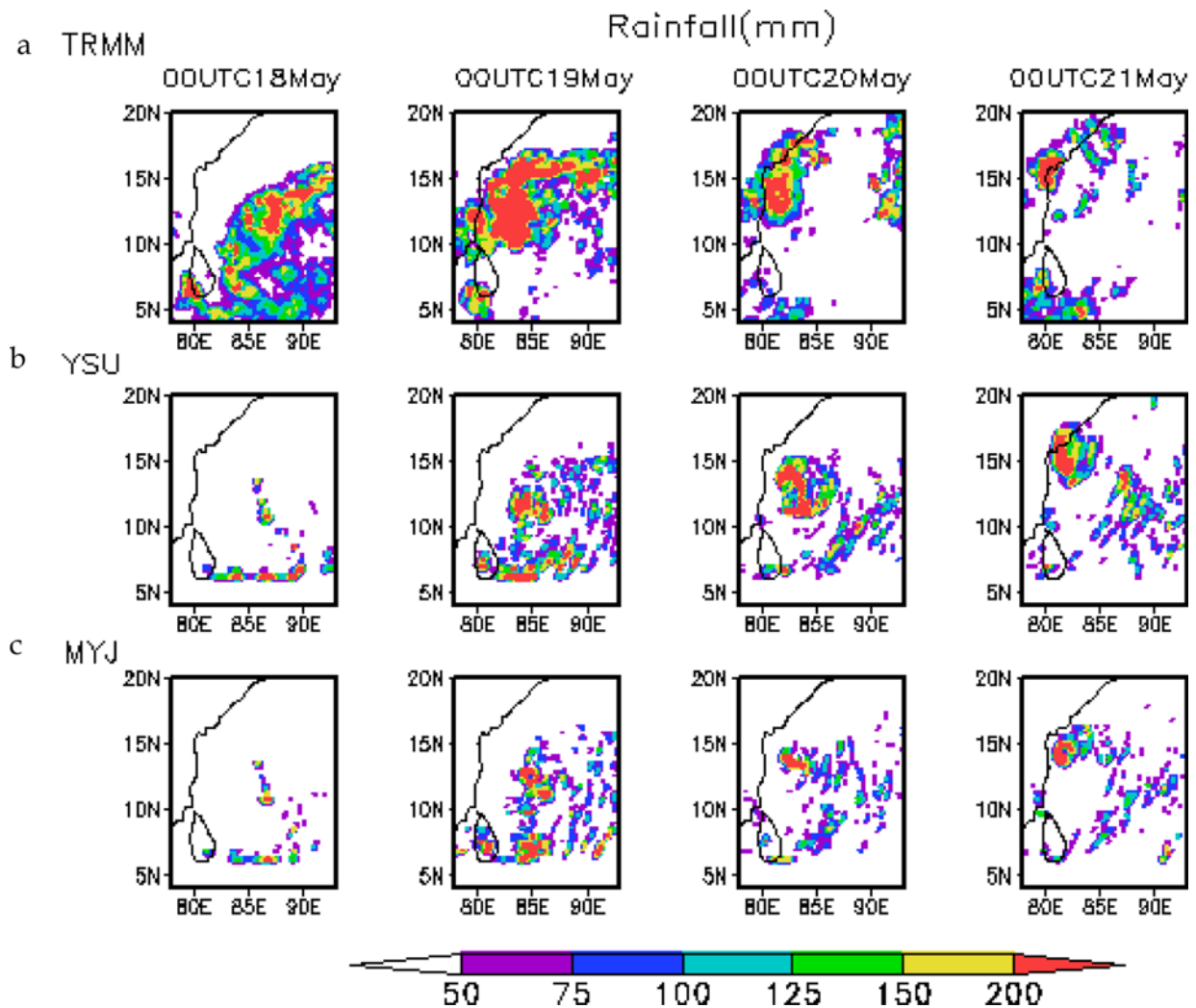


Fig. 10. Same as Fig. 6 but for PBL experiments.

agreement. For GD and Grell simulated storms, as intensity is underestimated, same is reflected in the rainfall patterns.

All these results show that the simulated track, intensity, precipitation patterns are sensitive to CPS. The only BMJ as CPS could simulate the track and intensity comparable to the observed one. The reason for better performance of BMJ may be due to proper representation of the large scale flow as well as the feedback mechanism which modulated this large scale flow by latent heat release. Whereas the large initial vertical wind shear inhibited the intensification of the storm in GD and Grell and large scale flow in KF simulated storm may have caused it to move away from the observed track. Thus, further experiments are conducted considering BMJ as CPS.

b. Sensitivity to PBL parameterization schemes

The second set of experiments consists of sensitivity of two PBL schemes such as YSU and MYJ. As discussed in the section 4.1, BMJ as CP and WSM6 as MP scheme are kept

fixed for these experiments.

The simulated track and intensity for these experiments along with IMD observations are presented in Figs. 7a-d. The direction of the movement of the storm is captured well by both the PBL schemes and the simulated tracks are overlapped with each other (Fig. 7a). The translational speed between the two modeled storms by YSU and MYJ is different and is clearly seen in Fig. 7a. The time evolution of the track error (Fig. 7b) shows similar and overlapped tracks up to 1200 UTC 20 May with maximum difference between the two simulated tracks is 50 km, thereafter the track error is drastically reduced for YSU storm. This increased difference between the two tracks simulated by YSU and MYJ is may be because of the slow translational speed of the MYJ storm. The intensity variation for LAILA cyclone is shown in Figs. 7c and d. The minimum CSLP variation (Fig. 7c) shows that both PBL schemes give overestimated intensity of the storm, but MYJ storm intensity is closer to the IMD observations. To elucidate the possible causes of these results, we have presented time

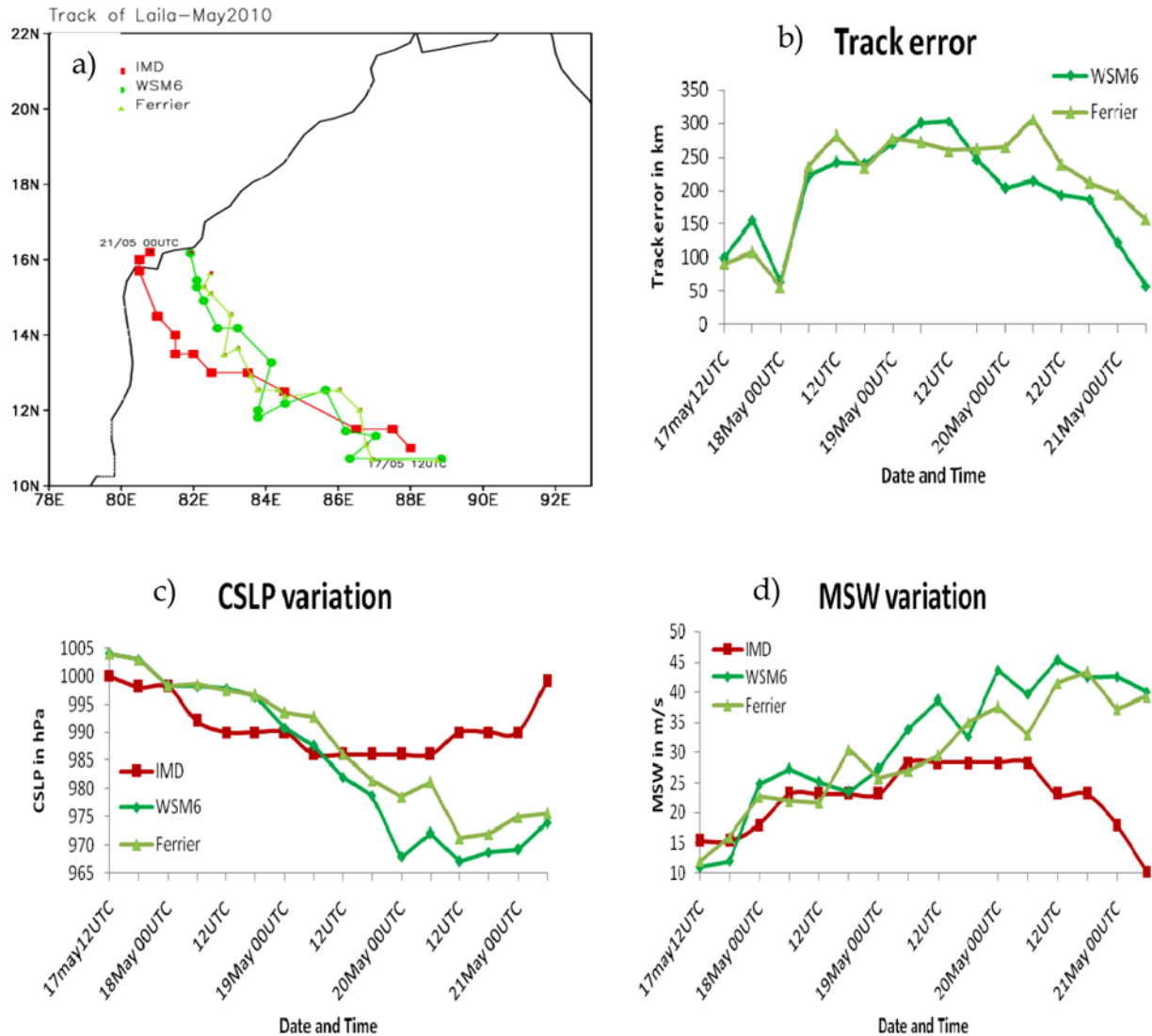


Fig. 11. Same as Fig. 2 but for the experiments with different microphysics parameterization (MP) schemes.

series of area averaged surface net heat flux (SNHF) in $W m^{-2}$ for cyclone LAILA in Fig. 8a. SNHF is sum of ground sensible heat flux (GR) and latent heat flux (LH). It is noted that the characteristic variations in SNHF are well in correspondence to the cyclone intensity variations. The higher values of SNHF correspond to the overestimated intensity by YSU and lower values of SNHF correspond to the closely matching intensity by MYJ with IMD observations. The latent heat flux (LH) is found to be more for YSU simulated storm than MYJ simulated storm (Fig. 8b). To further investigate the large disparity in the LH values the time evolution of relative humidity averaged over 5 degree around the storm center for the maximum intensity period (i.e., 1800 UTC 19 May to 0600 UTC 21 May) is shown in Fig. 8c for MYJ and YSU respectively. Eventhough the more relative humidity values at 0000 UTC 20 May are observed in MYJ simulated storm, relatively dry mid-troposphere is observed at this time. In YSU simulations, the boundary layer moisture is found to be more

along with high mid-tropospheric relative humidity. To explore the relation between the relative humidity and hydrometeor concentration, we have plotted (Figure not shown) the area averaged ($5^{\circ} \times 5^{\circ}$ around cyclone center) mixing ratio for each hydrometeor is plotted for MYJ and YSU. It shows that MYJ produced less condensates than YSU. Significant decrease in graupel and snow is noticed in MYJ. The radiosonde humidity profiles at Machilipatnam station are compared with model simulated humidity profile at 0000 UTC 19 May and at 0000 UTC 21 May (Fig. 9). MYJ simulations produce a moister boundary layer and lower troposphere while higher levels are significantly drier than YSU simulations. It can be seen that MYJ simulations maintain higher relative humidity at lower levels but above 800 hPa YSU provides a considerably larger moisture content. As expected the large amount of available moisture for condensation in YSU simulations may affects the vertical velocity fields and thus produces higher graupel and snow concentration resulting in higher intensity and vice versa

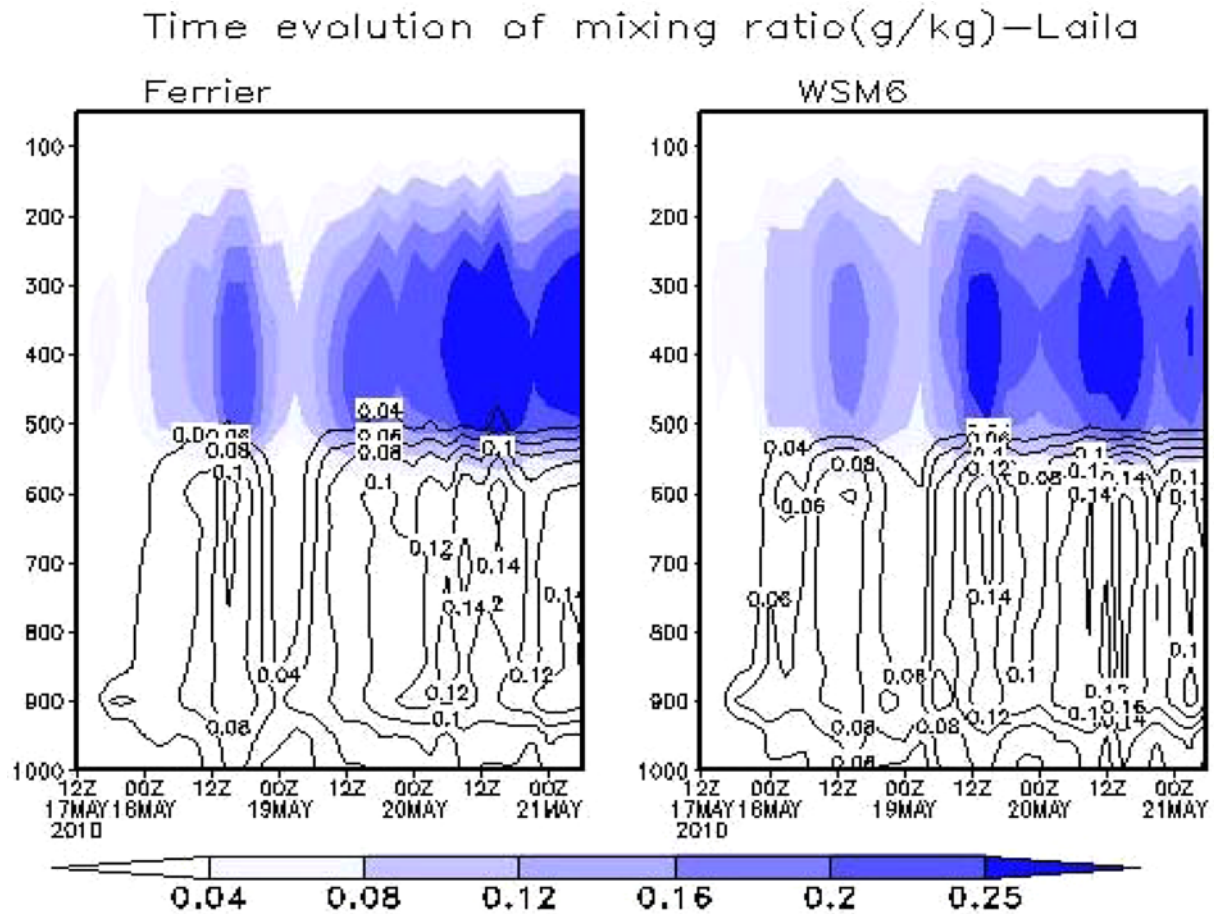


Fig. 12. Time evolution of area averaged mixing ratio in g kg^{-1} for Ferrier and WSM6 MP Schemes. The shaded are the frozen hydrometeors i.e., snow for Ferrier and ice, snow, graupel for WSM6 scheme. The contours represent the liquid hydrometeors i.e., rain water and cloud water.

in MYJ. In Fig. 9b, well matched humidity profiles for MYJ and YSU are observed. The YSU storm is close to the landfall with decreased intensity, while MYJ storm is still over the ocean and is far away from the station. It may be one of the reasons for similar humidity profiles for MYJ and YSU near landfall.

Higher values of relative humidity may indicate the favorable situation for deep mixing extended to the layer above the PBL top and thus moisture is transported upward through too deep of a layer, in YSU. While in MYJ, no mixing occurs with the air above the PBL and thus air in the PBL is mixed intensely among adjacent layers and hence low level moisture will be trapped in PBL resulting in the slow mixing. 24 hrs accumulated rainfall plotted at every 24 hrs interval starting from 0000 UTC 18 May for two PBL schemes along with the TRMM rainfall is shown in Fig. 10. The rainfall pattern and the surface track of cyclone simulated by MYJ and YSU are consistent with each other. Similarly the magnitudes of rainfall and intensity simulations by MYJ and YSU are matching very well with the TRMM observations.

It can be concluded from the above that the deepest vertical mixing in the simulations with YSU scheme, as illustrated by

the mean relative humidity (Fig. 8c) and vertical distribution of each hydrometeor (Figure not shown), resulted in more transfer of moisture from low to higher levels as well as latent heat release during the autoconversion processes of hydrometeors, further produced large amount of condensates (graupel and snow). Moreover, the reduced condensation at mid-levels due to limited water vapor supply, had a significant impact on latent heating affecting the intensity of the storm. MYJ scheme is a local closure scheme and many studies have reported that local schemes exhibit insufficient moisture transport at higher levels due to weak vertical mixing (Jankov et al., 2005, 2007; Hu et al., 2010). As a result, MYJ is usually too moist near the surface (Jankov et al., 2007; Hu et al., 2010). Another possible cause for the differences between YSU and MYJ runs would be the different surface layer schemes that are tied to each BL scheme. However, previous studies have shown (Hu et al., 2010; Shin and Hong, 2011) that surface layer parameterizations only contribute to near surface variability, whereas the shapes of the profiles are determined from the BL schemes. The role of free atmosphere diffusion in YSU was also examined by setting different values of mixing length (see Hong et al., 2006) which did not affect simulation results

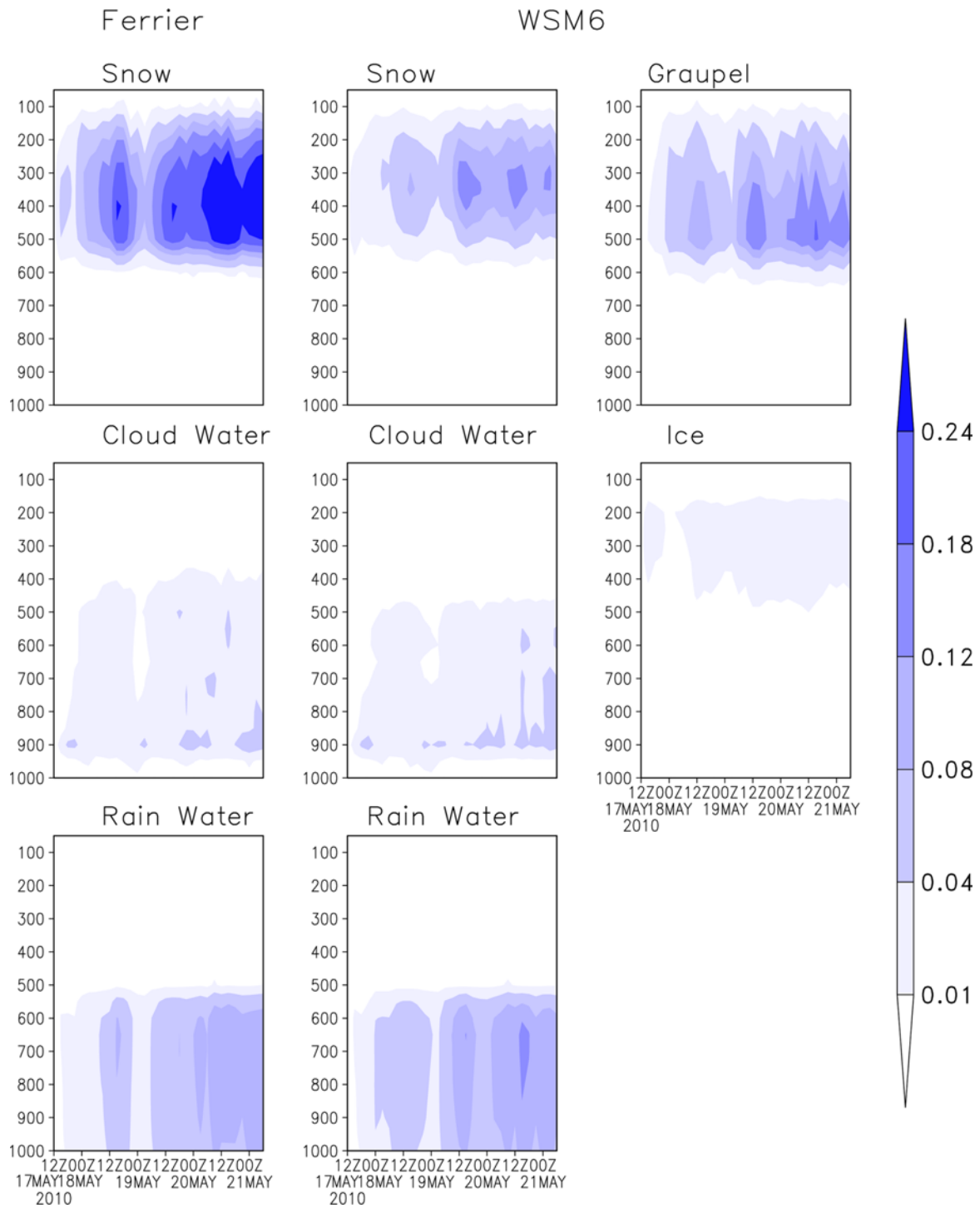


Fig. 13. Area Averaged Mixing ratio for each hydrometeor separately (a-c) for Ferrier and (d-h) for WSM6 MP schemes. a) and d) shows snow hydrometeor, b) and e) for cloud water, c) and f) shows rain water, g) graupel, and h) ice hydrometeor.

substantially (Figure not shown).

Keeping in view these results i.e., better simulation of track, translational speed and variations in the magnitude of the storm intensity, it is reasonable to say that YSU scheme performed better in the group. For next set of experiments, BMJ and YSU as CP and PBL scheme is kept fixed and

sensitivity of two microphysics schemes is conducted.

c. Sensitivity of microphysics parameterization schemes

The third group of experiments includes two experiments for sensitivity of microphysics scheme such as WSM6 and Ferrier.

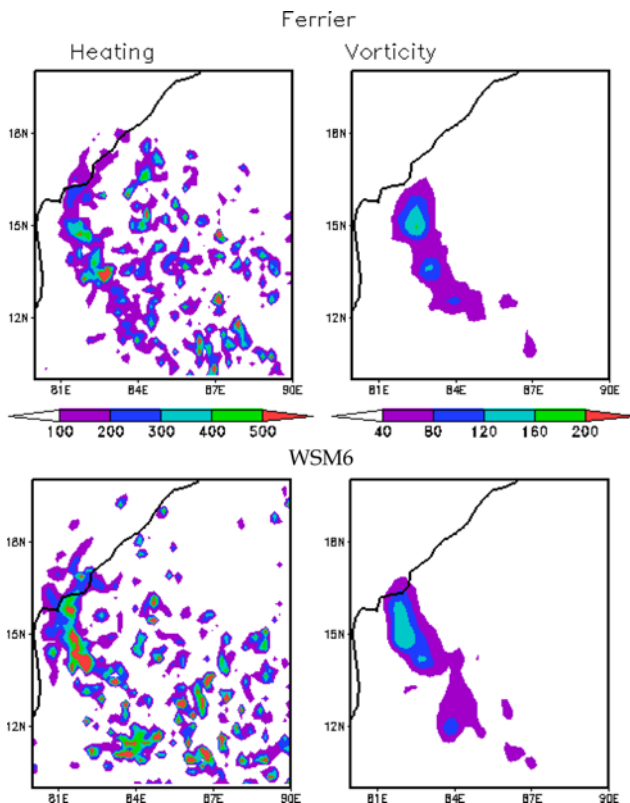


Fig. 14. Spatial distribution of a) middle level (500 hPa -300 hPa) heating (K Day^{-1}) b) Lower level (900-700 hPa) vorticity (10^{-5} s^{-1}) for Ferrier (upper panel) and WSM6 (lower panel), respectively.

Figures 11a-d show modeled track of cyclone LAILA, time evolution of track error in km and the intensity variation in terms of minimum CSLP and maximum surface winds along with IMD observation. The microphysics do not show much impact on the track of the cyclone, when it is over the ocean but when cyclone approaches towards the land, Ferrier show the stationary/stagnated cyclone (Fig. 11a). The modeled cyclone shows eastward bias in the track for both microphysics. The WSM6 modeled cyclone gave 12 hrs late landfall, whereas the Ferrier scheme failed to give the landfall and remains stationary over the ocean. The average track error for both schemes is less than 300 km and track error 24 hrs before observed landfall increases for Ferrier (Fig. 11b). The intensity of the cyclone LAILA is overestimated by both the schemes, but the Ferrier scheme is closer to the observed intensity. The difference between the intensity simulated by WSM6 and Ferrier is about 2-3 hPa (Fig. 11c). By taking into account the track and intensity both, the WSM6 has performed well. To know the reason behind the difference in the intensity simulation, the area averaged mixing ratio is plotted in Fig. 12. The frozen hydrometeors like snow for Ferrier and snow, graupel and ice for WSM6 are shaded and liquid hydrometeors like rain water and cloud water are shown in contours. The frozen hydrometeors have higher concentration at the respective mature stage of the cyclones for both Ferrier and

WSM6 experiments. It is shown by Lord et al. (1984, 1988), Mukhopadhyay et al. (2011), Kanase et al. (2014b) that, the auto conversion processes between the hydrometeors and the amount of latent heat released during this conversion is the main factor which controls the intensity of the cyclone. Here it is found that inspite of almost an equal amount of liquid hydrometeors; the intensity of the cyclone varies with the amount of frozen hydrometeors. Higher concentration of frozen hydrometeors in Ferrier gave lower intensity cyclone whereas comparatively lower concentration of frozen hydrometeors in WSM6 gave higher intensity of the cyclone. Here it is interesting to know the reason and thus type of the hydrometeor responsible for the intensity. Therefore we have plotted each hydrometeor separately (Fig. 13). For Ferrier scheme, snow is the only frozen hydrometeor while for WSM6 snow, graupel and ice are the frozen hydrometeors. Snow is present at 400 hPa. Ice (which is present above 300 hPa) and snow are aligned at the leading edge of the system. Graupel is found in the middle tropospheric level (~ 500 hPa) and rainwater and cloud water below the freezing level. In Ferrier, the snow mixing ratio is found to be more, whereas in WSM6, the snow mixing ratio is found to be decreased but the graupel concentration is more than snow concentration. Thus the presence of large amount of graupel in the mid-troposphere may produces large latent heat which may have contributed towards the increased intensity in WSM6 simulated storm. The liquid hydrometeors such as cloud and rain water in both WSM6 and Ferrier simulated storm remains more or less unchanged and hence may not affect the intensity. The ice concentration in WSM6 is found to be very less and may not be contributing towards the intensity of the cyclone. Thus the lowered generation of snow and higher production of graupel in WSM6 could be an indication of overestimated cyclone intensity.

To explore the relation between the heating and cyclone intensity further, the spatial distribution of middle level (500-300 hPa) heating and lower level (900-700 hPa) vorticity are computed for Ferrier and WSM6 (Fig. 14) respectively. It is clearly seen that the locus of maximum vorticity followed the region of organized and coherent heating in Ferrier and WSM6. It is also evident from Fig. 14 that the higher concentration of snow in Ferrier has produced less mid-tropospheric heating, while lower snow concentration and higher graupel concentration in WSM6 have produced more heating in the mid-troposphere, which may have contributed towards the higher intensity values in WSM6. To demonstrate the role of hydrometeors on the forecast deviation, the percentage contribution of each hydrometeor is plotted for MP experiment (Figure not shown). Snow, rainwater and graupel show a similar pattern and the same location as that of the middle level heating in Ferrier and WSM6. The path of maximum ice and cloud water do not coincide with the path of maximum heating. Thus, it appears that the generation of snow along with increased amount of graupel around the cyclone center in WSM6 plays an important role in modulating the

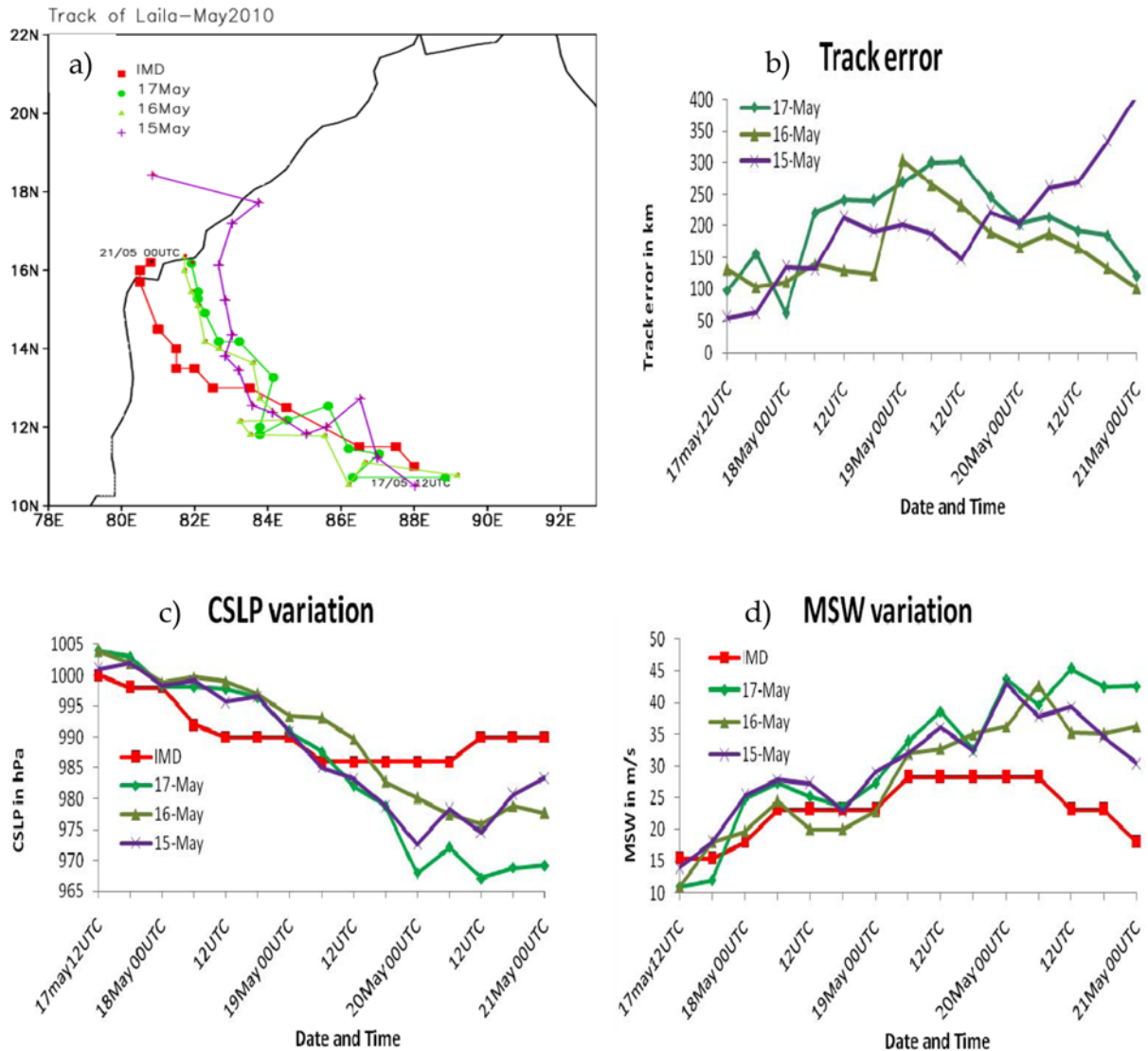


Fig. 15. Same as Fig. 2 but for the experimnets with different initial conditions such as 0000 UTC 15 May, 0000 UTC 16 May, and 0000 UTC 17 May with fixed combination BMJ-YSU-WSM6 as CP-PBL-MP schemes.

middle level heating which in turn influences the instability and thus the intensity of modeled cyclone. 24 hrs accumulated rainfall in mm at every 24 hrs interval starting from 0000 UTC 18 May for Ferrier and WSM6 show well matched magnitudes and rainfall pattern with TRMM observations (Figure not shown)

d. Sensitivity to initial and boundary conditions

Thus the results discussed from section 4. a to section 4. c suggest that the combination BMJ-YSU-WSM6 of Cumulus, PBL and microphysics scheme gave better track and intensity forecast for cyclone LAILA. Therefore to study the sensitivity of initial and boundary conditions, this combination is kept fixed and two initial conditions such as 0000 UTC 16 May referred as 16 May and 0000 UTC 15 May (15 May) in

addition to 0000 UTC 17 May (17 May) are used. The initial condition 15 May is 24 hrs before the low pressure area (LoPar), 16 May is LoPar and 17 May is the initial condition which is 6 hrs before formation of depression.

The modeled surface track of cyclone LAILA plotted with IMD observed track, time evolution of track error in km and the intensity variation in terms of minimum CSLP and maximum surface winds are shown in Figs. 15a-d. For first 5days from 15may as IC, the track error lies below 200 km and after that track error continuously increases. It may be because WRF model has ability to produce the genesis and hence the depression stage as seen from Fig. 15a. For 16 May and 17 May, the location of the depression stage is close to each other but far away from the IMD observed position. Eventhough the model simulated surface tracks for 16 May and 17 May, seems to be overlapped with each other, the track error is found to be

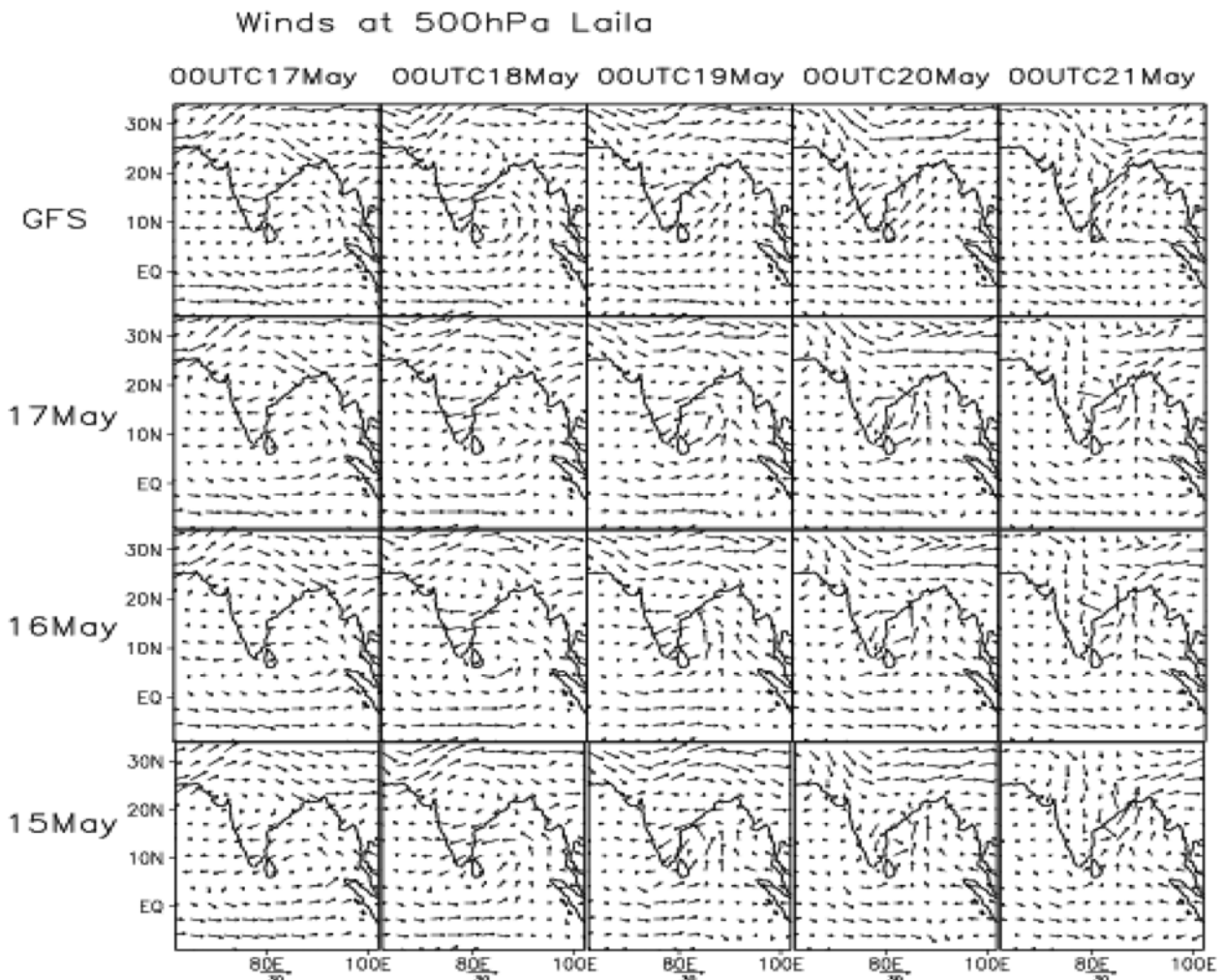


Fig. 16. Wind fields at 500 hPa level for GFS and three initial condition sensitivity experiments with every 24 hrs of interval from 0000 UTC 17 May for cyclone LAILA. Upper panel-GFS, second panel-0000 UTC 17 May, third panel: 0000 UTC 16 May and lower most panel: 0000 UTC 15 May as initial condition.

minimum for 16 May whereas for 17 May, it has large deviation from the IMD track (Fig. 15b) which may be due to the slow translational speed of modeled cyclone. For all the three initial conditions, modeled storm showed late landfall. The observed storm is reached close to land on 20 May whereas the modeled storms (with three initial conditions) are still away from the coast. At 0000 UTC 21 May, the observed storm was over land, but the modeled storms are still over the ocean surface, which caused it to remain intensified till 21 May. The small variation in the mid tropospheric flow may be responsible for the variation in the track error (Fig. 16). The mid-tropospheric flow at 500 hPa for GFS qualitatively matches well with 17 May and 16 May experiments and for 15 May more eastward bias observed with respect to the center of the system. The smaller changes in the surface initial position has led to the significant changes in mid-tropospheric temperature and humidity (Figure not shown) throughout the time integration period and may be responsible for the intensity change with fixed MP and PBL schemes. The intensity is

overestimated with all the initial conditions, but with 16 May it is closer to the IMD observed intensity (Figs. 15c, d). To understand the variation in the intensity we have examined temporal evolution of area averaged mixing ratio in Fig. 17. Maximum concentration of frozen hydrometeors persists for longer time for 17 May and 15 May and for less time for 16 May. Thus, auto conversion processes in 17 May and 15 May have lasted longer than 16 May and thus increased latent heat release caused increase in the mid-tropospheric temperature and the positive feedback is resulted in increased intensity. To establish the role of hydrometeors on intensity simulation, we have plotted the area averaged mixing ratio of each hydrometeor separately for three ICs (Figure not shown). It is clearly demonstrated that the changing concentration of graupel has more profound impact on the intensity than the snow hydrometeor. Figure 18 shows the mid-tropospheric heating and lower level vorticity for 17 May, 16 May and 15 May as Initial conditions. The locus of maximum vorticity is followed by the maximum mid-tropospheric heating. For 15 May

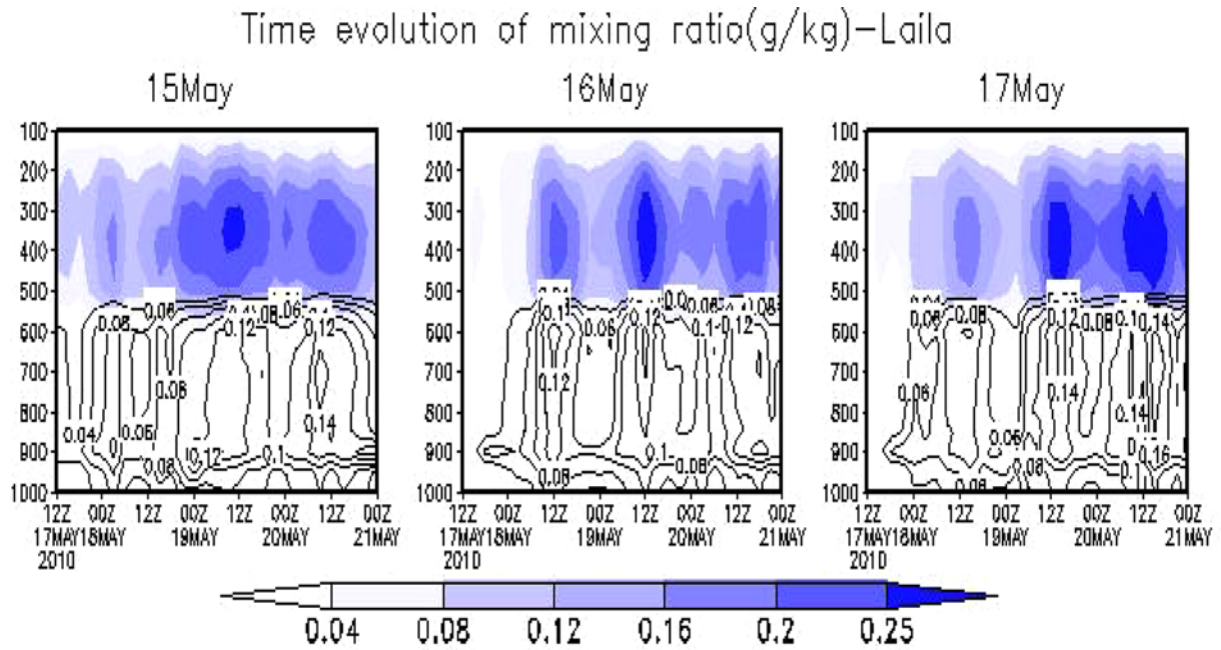


Fig. 17. Same as Fig. 10 but for initial condition sensitivity experiments i.e., 15 May, 16 May, and 17 May respectively for cyclone LAILA.

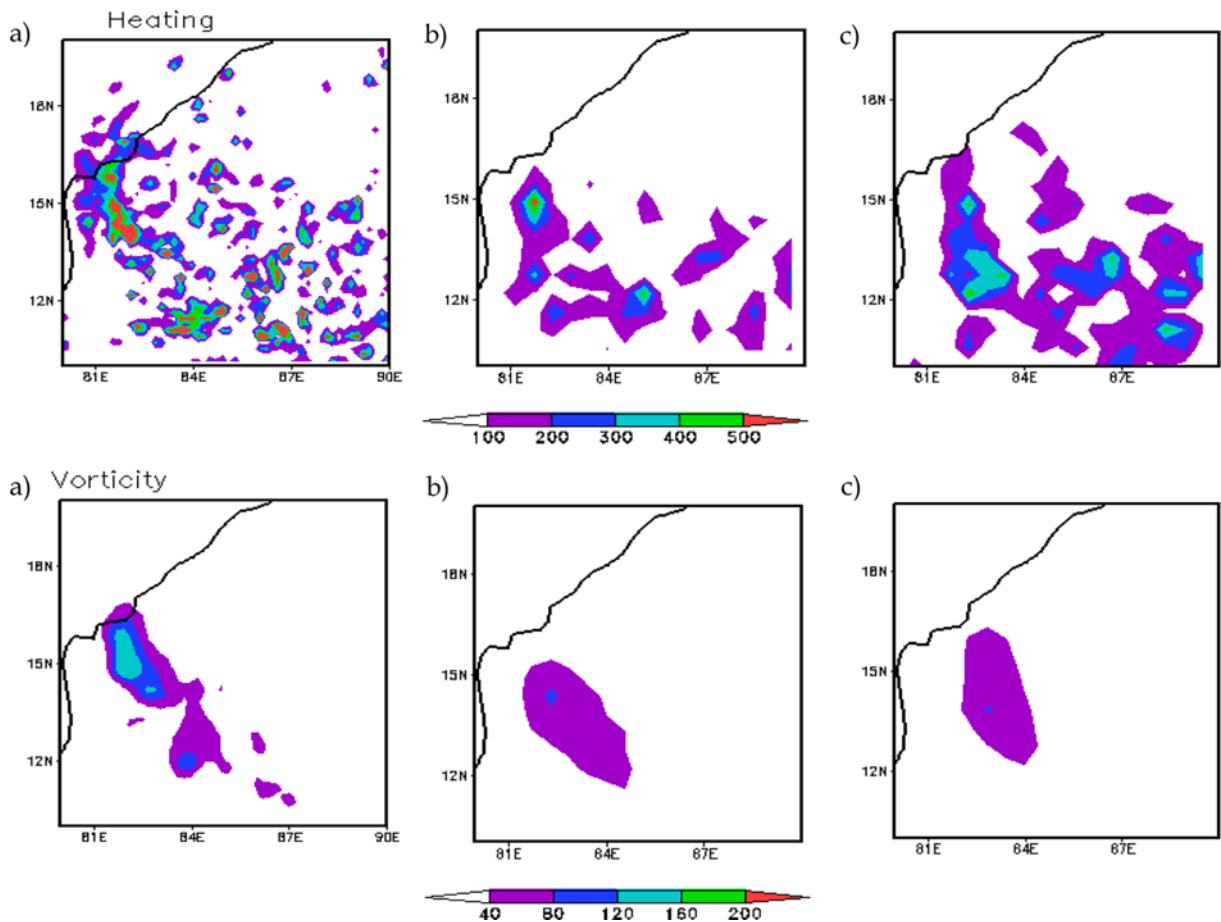


Fig. 18. Same as Fig. 14 but for IC sensitivity experiments for a) 17 May, b) 16 May, and c) 15 May.

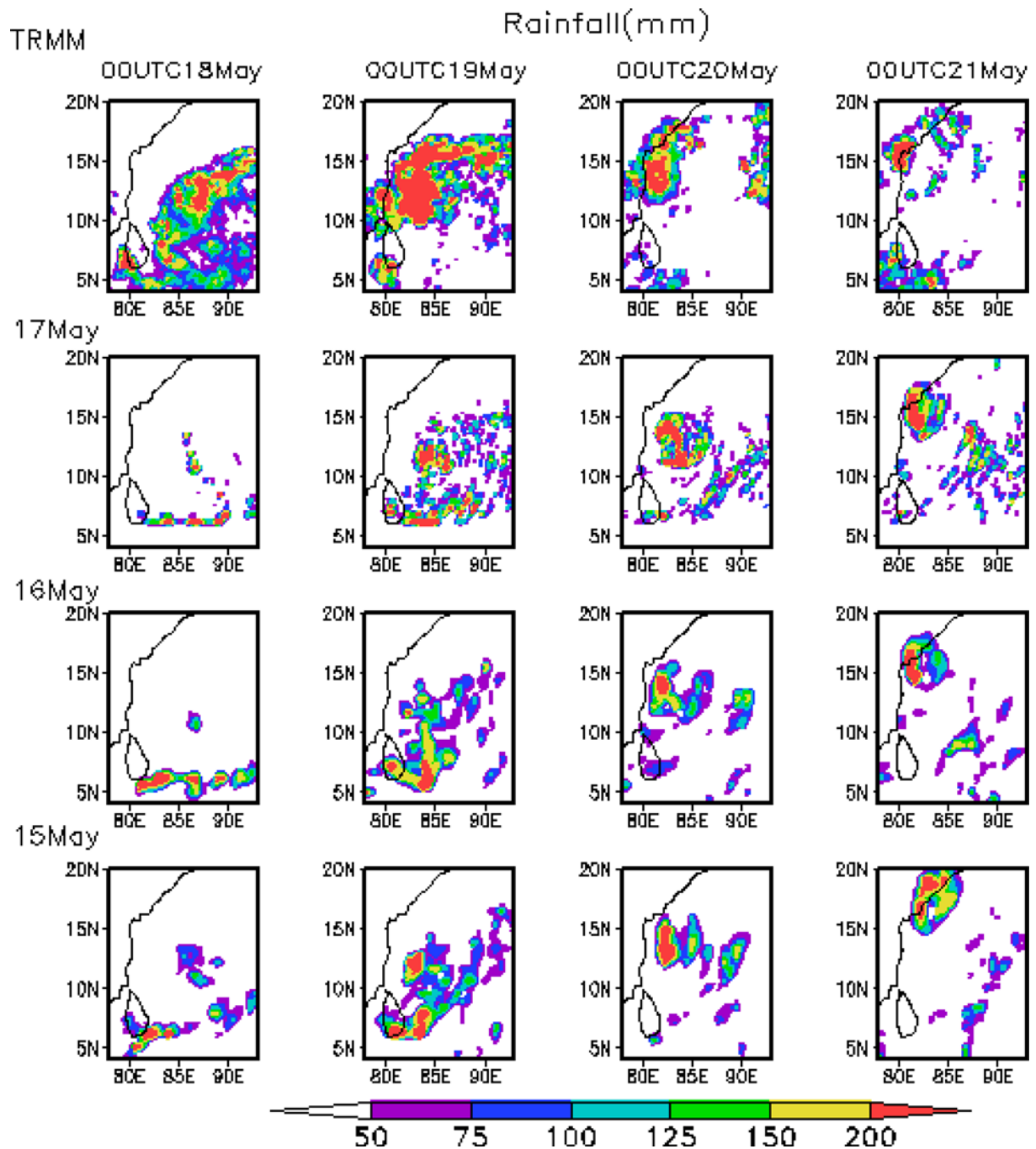


Fig. 19. Same as Fig. 6 but for IC sensitivity experiments.

experiment, the lowered values of lower vorticity corresponds to the lowered mid-tropospheric heating. Similarly for 17 May, higher values of vorticity correspond to the higher middle level heating leading to higher intensity. Increased lower level vorticity pumps more moisture from the ocean surface causing positive feedback and thus more intense storm in 17 May. The mid-tropospheric warming and lower level vorticity values are less in 16 May and 15 May experiments causing relatively less intense storms. For 16 May, the proper representation of mid-level heating corresponds to the intensity values closer to IMD

observations. Thus, depending upon the mid-tropospheric heating (which may acts as the driver for the moisture pumping from lower levels to higher levels) intensity of each cyclone varies. 24 hrs accumulated rainfall (Fig. 19) plotted for three IC experiments such as 17 May, 16 May and 15 May along with TRMM observations show that the intensity of the modeled storm and the simulated rainfall amount are in close agreement, whereas 16 May experiment has well matched rainfall pattern as well as magnitudes of rainfall close to TRMM observations.

5. Conclusions

Our results suggest physical parameterization in WRF-ARW model have large sensitivity on intensity and track of severe cyclonic storm LAILA. The track and intensity of the storm is also very sensitive to the initial conditions and thus the intensity of the vortex. Here an attempt is also being made to elucidate possible mechanisms for intensity modulation.

The cumulus parameterization experiments suggest that BMJ scheme has produced the best track and both BMJ and KF have produced more intense storm while GD and Grell have lower intensity storm. The impact of CP schemes on large scale environment is well demonstrated from CP sensitivity experiments. The mid-tropospheric flow (at 500 hPa) for GFS and BMJ are in close agreement with each other, whereas strengthened northward flow and interaction with the mid-latitude westerlies caused KF storm to move to the east side of the observed storm. The GD and Grell schemes failed to produce the cyclonic circulation at 500 hPa and hence produced lower intensity and dissipated very fast. The higher wind shear values at initial stage may have inhibited the further intensification of the cyclone in GD and Grell, while lower values of shear may have helped to form a more intense storm in BMJ and KF. A well developed storm in BMJ and KF may be able to sustain the increased shear values. The inner core rainfall of storms is a good indicator of the latent heat release, which is a crucial heat source for intensification and the rainfall intensity is significantly correlated with the intensity of the storms. The BMJ and KF are able to produce more realistic pattern of 24 hrs accumulated rainfall than GD and Grell. Thus, only BMJ as CPS could simulate the track and intensity of LAILA, comparable with the observations. The reason for better performance of BMJ may be proper representation of the large scale flow as well as the feedback mechanism which modulated this large scale flow by latent heat release.

The PBL sensitivity experiments indicate that all the simulated tracks have less track error compared to CPS experiments. The track and the translational speed of the storm are well simulated by the YSU scheme while the intensity simulated by MYJ is close to the IMD observation. The further investigation of the temporal evolution of the area averaged total surface net heat fluxes (SNHF) explores the higher SNHF is associated with the more intense storm in YSU and vice versa. This is investigated further with the help of time evolution of latent heat flux and relative humidity. In YSU, the deep mixing extended to the layer above the PBL top and thus moisture is transported upward through too deep of a layer, while in MYJ, no mixing occurs with the air above the PBL while air in the PBL is mixed intensely among adjacent layers and hence low level moisture will be trapped in PBL resulting in the slow mixing and thus causing lower intensity storms in MYJ. The rainfall pattern in YSU is also in close agreement with TRMM observations. Thus YSU as PBL scheme performs better in this group.

The MPS sensitivity experiments shows insignificant impact on the track of the cyclone, but the intensity is largely affected by the MP scheme. The frozen hydrometeor concentration and thus the latent heat released during the auto-conversion processes are responsible for the intensity of the storm. It is found that the WSM6 is able to produce a realistic feature of the cyclones as compared to the other schemes. The relative success of this scheme is attributed to its ability in incorporating an improved snow/graupel production by weighted mixing ratio and rain auto conversion process. The ice and graupel concentration is much lower near the cyclone center. Ice is abundant in the higher levels near the leading edge of the outflow. The snow is the hydrometeor with maximum contribution (found at ~400 hPa) followed by rainwater in the lower levels. Cyclone intensity is strongly influenced by heating within it and the heating is dominantly influenced by the snow and graupel production within the cyclone environment. So the vertical distribution as well as the spatio-temporal distribution of snow and graupel (Mukhopadhyay et al., 2011) and thus the mixed phase hydrometeors in WSM6 is the decisive factor for cyclone intensity forecasts over the Indian Ocean

The last set of experiments dealt with the sensitivity to initial conditions and boundary conditions. The small differences in the initial wind fields are resulted in the remarkable changes in the track and intensity of the storm. Impact of large scale flow is clearly demonstrated with the help of 500 hPa wind fields. The wind shear values at the initial stage plays an important role in determining the intensity of the cyclone. The concentration of the frozen hydrometeors especially snow and graupel, their time of persistence along with the realistic representation of mid-tropospheric heating, well matched rainfall pattern in 16 May experiment are the important factors responsible for determining the intensity of LAILA close to IMD observations.

In general we note that the track and intensity is more sensitive to CPS schemes, but the MPS and PBL schemes also has impact on the intensity of the cyclones. Thus choosing the appropriate CP scheme in model will greatly influence the track of the cyclone and thus will minimize the track error. In addition to the appropriate CP scheme, the choice of PBL and MPS scheme will also lead to the better intensity simulation. The change in the initial and boundary conditions also have remarkable impact on the track and intensity of the cyclone. We feel that more research on the sensitivity to initial and boundary conditions is required to come to a firm conclusion. We understand that one case study might not be able to substantially support the findings; however, we strongly feel that findings of this work will definitely supplement the current understanding of weak intensity cyclones. In future, we would like to study the impact of different intensity vortices as initial conditions on track and intensity of the weak intensity storms.

Acknowledgments. The authors wish to thank the Director, Indian Institute of Tropical Meteorology (IITM), Pune for his encouragement and support. Authors acknowledge the use of

WRF-ARW model, which is made available on the Internet by the Mesoscale and Microscale division of NCAR. The use of GFS data, RTG-SST data, IMD observations and GrADS software is acknowledged with thanks. The authors acknowledge the Korean Meteorological Society for supporting the publication fee.

Edited by: Jimy Dudhia

REFERENCES

- Anthes, R. A., Y. Kuo, S. Benjamin, and Y. F. Li, 1982: The evolution of the mesoscale environment of severe local storms: preliminary modeling results. *Mon. wea. Rev.*, **110**, 1187-1213.
- Arpe, K., A. Hollingsworth, M. S. Tracton, A. C. Lorenc, S. Uppala, and P. Kallberg, 1985: The response of numerical weather prediction systems on the FGGE level IIb data. Part 2: Forecast verifications and implications for predictability. *Quart. J. Roy. Meteor. Soc.*, **111**, 67-101.
- Betts, A. K., 1986: A new convective adjustment scheme Part I: Observational and theoretical basis. *Quart. J. Roy. Meteor. Soc.*, **112**, 677-691.
- _____, and M. J. Miller, 1986: A new convective adjustment scheme Part II: Single column tests using GATE wave, BOMEX, and arctic air mass data sets. *Quart. J. Roy. Meteor. Soc.*, **112**, 693-709.
- Bhaskar Rao, D. V., and D. Hari Prasad, 2006: Numerical prediction of the Orissa super cyclone (1999): Sensitivity to the parameterization of convection, boundary layer and explicit moisture processes. *Mausam*, **57**, 61-78.
- _____, and _____, 2007: Sensitivity of tropical cyclone intensification to boundary layer and convective processes. *Nat. Hazards*, **41**, 429-445.
- _____, _____, and D. Srinivas, 2009: Impact of horizontal resolution and the advantages of the nested domains approach in the prediction of tropical cyclone intensification and movement. *J. Geophys. Res.*, **114**, D11106, 1-24.
- Cacciamani, C., D. Cesari, F. Grazzini, T. Paccagnella, and M. Pantone, 2000: Numerical simulation of intense precipitation events south of the Alps: Sensitivity to initial conditions and horizontal resolution. *Meteor. Atmos. Phys.*, **72**, 147-159.
- Charney, J. G., and A. Eliassen, 1964: On the growth of the hurricane depression. *J. Atmos. Sci.*, **21**, 68-75.
- Deshpande, M., S. Pattanaik, and P. S. Salvekar, 2010: Impact of physical parameterization schemes on numerical simulation of super cyclone Gonu. *Nat. Hazards*, **55**, 211-231.
- _____, _____, and _____, 2012: Impact of cloud parameterization on the numerical simulation of a super cyclone. *Ann. Geophys.*, **30**, 775-795.
- Dudhia, J., 1989: Numerical study of convection observed during the winter monsoon experiment using a mesoscale two-dimensional model. *J. Atmos. Sci.*, **46**, 3077-3107.
- _____, S.-Y. Hong, and K. S. Lim, 2008: A new method for representing mixed-phase particle fall speeds in bulk microphysics parameterizations. *J. Meteor. Soc. Japan*, **86A**, 33-44.
- Efstathiou, G. A., N. M. Zoumakis, D. Melas, and P. Kassomenos, 2012 : Impact of precipitating ice on the simulation of heavy rainfall event with advanced research WRF using two bulk microphysical schemes. *Asia-Pac. J. Atmos. Sci.*, **48**, 357-368.
- _____, _____, _____, and _____, 2013: Sensitivity of WRF to boundary layer parameterizations in simulating a heavy rainfall event using different microphysical schemes. Effect on large-scale processes. *Atmos. Res.*, **132-133**, 125-143, <http://dx.doi.org/10.1016/j.atmosres.2013.05.004>.
- Emanuel, K. A., 1986: An air-sea interaction theory for tropical cyclones. Part I: Steady state maintenance. *J. Atmos. Sci.*, **43**, 585-604.
- _____, 2004: Tropical cyclone energetics and structure. *Atmospheric Turbulence and Mesoscale Meteorology*, edited by: Federovich, E., Rotunno, R., and Stevens, B., Cambridge University Press, 165-192.
- _____, J. D. Neelin, and C. S. Bretherton, 1994: On large scale circulations of convecting atmospheres. *Quart. J. Roy. Meteor. Soc.*, **120**, 1111-1143.
- Frank, W. M., and E. A. Ritchie, 2001: Effects of vertical wind shear on the intensity and structure of numerically simulated hurricanes. *Mon. Wea. Rev.*, **129**, 2249-2269.
- Gray, W. M., 1968: Global view of the origin of tropical disturbances and storms. *Mon. Wea. Rev.*, **96**, 669-700.
- Grell, G. A., and D. Devenyi, 2002: A generalized approach to parameterizing convection combining ensemble and data assimilation techniques. *Geophys. Res. Lett.* **29**, 14, 38-138-4, doi:10.1029/2002-GL015311.
- Hill, K. V., and G. M. Lackman, 2009: Analysis of idealized tropical cyclone simulations using the Weather Research and Forecasting Model: Sensitivity to turbulence parameterization and grid spacing. *Mon. Wea. Rev.*, **137**, 745-765.
- Hong, S.-Y., and J.-O. J. Lim, 2006: The WRF Single-Moment 6-Class Microphysics Scheme (WSM6). *J. Korean Meteor. Soc.*, **42**, 129-151.
- _____, Y. Noh, and J. Dudhia, 2006: A new vertical diffusion package with an explicit treatment of entrainment processes. *Mon. Wea. Rev.*, **134**, 2318-2341.
- _____, and H.-L. Pan, 1996: Nonlocal boundary layer vertical diffusion in a medium range forecast model. *Mon. Wea. Rev.* **124**, 2322-2339.
- Hu, X.-M., J. W. Nielsen-Gammon, and F. Zhang, 2010: Evaluation of three planetary boundary layer schemes in the WRF model. *J. Appl. Meteor. Climatol.*, **49**, 1831-1844.
- Janjic, Z. I., 1990 : The step-mountain coordinate: physical package. *Mon. Wea. Rev.*, **118**, 1429-1443.
- _____, 1996: The surface layer in the NCEP Eta Model. Eleventh Conference on Numerical Weather Prediction. Norfolk, VA, 19-23 August. American Meteorology Society Boston, MA, 354-355.
- _____, 2000: Comments on "Development and evaluation of a convection scheme for use in climate models". *J. Atmos. Sci.*, **57**, 3686.
- _____, 2002: Nonsingular Implementation of the Mellor-Yamada Level 2.5 Scheme in the NCEP Meso Model. NCEP Office Note 437, 61.
- Jankov, I., W. A. Gallus, M. Segal, B. Shaw, and S. E. Koch, 2005: The impact of different WRF model physical parameterizations and their interactions on warm season MCS rainfall. *Wea. Forecasting*, **20**, 1048-1060.
- _____, P. J. Schultz, C. J. Anderson, and S. E. Koch, 2007: The impact of different physical parameterizations and their interactions on cold season QPF in the American River Basin. *J. Hydrometeorol.*, **8**, 1141-1151.
- Kain, J. S., 2004: The Kain-Fritsch convective parameterization: An update. *J. Appl. Meteorol.*, **43**, 170-181.
- Kanase, R. D., and P. S. Salvekar, 2014a: Study of weak intensity cyclones over bay of Bengal using WRF model. *Atmos. Climate Sci.*, **4**, 534-548.
- _____, P. Mukhopadhyay, and P. S. Salvekar, 2014b: Understanding the role of cloud and convective process in simulating the weaker cyclones over Indian Seas. *Pure Appl. Geophys.*, doi:10.1007/s00024-014-0996-3.
- Kuo, Y.-H., and R. J. Reed, 1988: Numerical simulation of an explosively deepening cyclone in the eastern Pacific. *Mon. Wea. Rev.*, **116**, 2081-2105.
- Li, X., and Z. Pu, 2008: Sensitivity of numerical simulation of early rapid intensification of Hurricane Emily (2005) to cloud microphysical and planetary boundary layer parameterizations. *Mon. Wea. Rev.*, **136**, 4819-4838.
- Lord, S. J., and J. M. Lord, 1988: Vertical velocity structure in an axisymmetric, nonhydrostatic tropical cyclone model. *J. Atmos. Sci.*, **45**, 1453-1461.
- _____, H. E. Willoughby, and J. M. Piotrowicz, 1984: Role of a

- parameterized ice-phase microphysics in an axisymmetric, non-hydrostatic tropical cyclone model. *J. Atmos. Sci.*, **41**, 2836-2848.
- Lorenz, E. N., 1963: Deterministic nonperiodic flow. *J. Atmos. Sci.*, **20**, 130-141.
- Mellor, G. L., and T. Yamada, 1982: Development of a turbulence closure model for geophysical fluid problems. *Rev. Geophys. Space Physics*, **20**, 851-875.
- Merrill, R. T., 1988: Environmental influence on Hurricane intensification. *J. Atmos. Sci.*, **45**, 1678-1687.
- Mlawer, E. J., S. J. Taubman, P. D. Brown, M. J. Iacono, and S. A. Clough, 1997: Radiative transfer for inhomogeneous atmosphere: RRTM, a validated correlated-k model for the longwave. *J. Geophys. Res.*, **102**, 16663-16682.
- Mohanty, U. C., K. K. Osuri, A. Routray, M. Mohapatra, and S. Pattanayak, 2010: Simulation of bay of Bengal tropical cyclones with WRF model: Impact of initial and boundary conditions. *Mar. Geod.*, **33**, 294-314.
- Montgomery, M. T., and R. K. Smith, 2011: Paradigms for tropical-cyclone intensification. *Quart. J. Roy. Meteor. Soc.*, **137**, 1-31.
- _____, J. Persing, and R. K. Smith, 2015: Putting to rest WISHE-ful misconceptions for tropical cyclone intensification. *J. Adv. Modeling Earth Syst.*, **7**, 92-109, doi:10.1002/2014MS000362.
- _____, S. V. Nguyen, R. K. Smith, and J. Persing, 2009: Do tropical cyclones intensify by WISHE?. *Quart. J. Roy. Meteor. Soc.*, **135**, 1697-1714.
- Mullen, S. L., and D. P. Baumhefner, 1989: The impact of initial condition uncertainty on numerical simulations of large scale explosive cyclogenesis. *Mon. Wea. Rev.*, **117**, 2800-2821.
- Mukhopadhyay, P., S. Taraphdar, and B. N. Goswami, 2011: Influence of moist processes on track and intensity forecast of cyclones over the north Indian Ocean. *J. Geophys. Res.*, D05116, doi:10.1029/2010-JD014700.
- Osuri, K. K., U. C. Mohanty, A. Routray, M. A. Kulkarni, and M. Mohapatra, 2012: Customization of WRF-ARW model with Physical parameterization schemes for the simulation of tropical cyclones over North Indian Ocean. *Nat. Hazards*, **63**, 1337-1359.
- _____, U. C. Mohanty, A. Routray, M. Mohapatra, and D. Nivogi, 2013: A real-time track prediction of tropical cyclones over the North Indian Ocean using the ARW model. *J. Appl. Meteor. Climatol.*, **52**, 2476-2492.
- Pattanaik, D. R., and Y. V. Rama Rao, 2009: Track prediction of very severe cyclone 'Nargis' using high resolution weather research forecasting (WRF) model. *J. Earth Syst. Sci.*, **118**, 4, 309-329.
- Pattanayak, S., and U. C. Mohanty, 2008: A comparative study on performance of MM5 and WRF models in simulation of tropical cyclones over Indian seas. *Curr. Sci. India*, **95**, 923-936.
- Pielke, R. A., and Coauthors, 2006: A new paradigm for parameterizations in numerical weather prediction and other atmospheric models. *Natl. Wea. Digest*, **30**, 93-99.
- Raju, P. V. S., J. Potty, and U. C. Mohanty, 2011: Sensitivity of physical parameterizations on prediction of tropical cyclone Nargis over the Bay of Bengal using WRF model. *Meteor. Atmos. Phys.*, **113**, 125-137.
- Ritchie, E. A., 2002: Topic 1.2: Environmental effects. Topic Chairman and Rapporteur Report. The 5th WMO International Workshop on Tropical Cyclones IWTC-V, WMO Tech. Doc. WMO TD 1136.
- Rodgers, E. B., J. J. Baik, and H. F. Pierce, 1994a: The environmental influence on tropical cyclone precipitation. *J. Appl. Meteorol.*, **33**, 573-593.
- _____, S. W. Chang, and H. F. Pierce, 1994b: A satellite observational and numerical study of precipitation characteristics in western North Atlantic tropical cyclones. *J. Appl. Meteorol.*, **33**, 129-139.
- Ross, R. J., and Y. Kurihara, 1995: A numerical study on influence of Hurricane Gloria (1985) on the environment. *Mon. Wea. Rev.*, **123**, 332-346.
- RSMC Report, 2011: A report on cyclonic disturbances over North Indian Ocean during 2010. New Delhi, India, India Meteorological Department.
- Sanders, F., 1987: Skill of NMC operational models in prediction of explosive cyclogenesis. *Wea. Forecasting*, **2**, 322-336.
- Shin, H. H., and S.-Y. Hong, 2011: Intercomparison of planetary boundary-layer parameterizations in the WRF model for a single day from CASES-99. *Bound.-Layer Meteorol.*, **139**, 261-281.
- Skamarock, W. C., J. B. Klemp, J. Dudhia, D. Gill, D. Barker, W. Wang, X. Y. Huang, and J. G. Powers, 2008: A description of the advanced research WRF version 3, NCAR Technical Note, 475.
- Smith, R. K., 1997: On the theory of CISK. *Quart. J. Roy. Meteor. Soc.*, **123**, 407-418.
- Srinivas, C. V., R. Venkatesan, D. V. Bhaskar Rao, and D. Hari Prasad, 2007: Numerical simulation of Andhra severe cyclone (2003). model sensitivity to the boundary layer and convective parameterization. *Pure Appl. Geophys.*, **164**, 1465-1487.
- _____, _____, V. Yesubabu, and C. Nagaraju, 2010: Impact of assimilation of conventional and satellite meteorological observations on the numerical simulation of a Bay of Bengal tropical cyclone of Nov 2008 near Tamilnadu using WRF model. *Meteor. Atmos. Phys.*, **110**, 19-44.
- _____, D. V. Bhaskar Rao, V. Yesubabu, R. Baskarana, and B. Venkatraman, 2013: Tropical cyclone predictions over the Bay of Bengal using the high-resolution Advanced Research Weather Research and Forecasting (ARW) model. *Quart. J. Roy. Meteor. Soc.*, **139**, 1810-1825.
- Srinivas D., and D. V. Bhaskar Rao, 2014: Implications of vortex initialization and model spin-up in tropical cyclone prediction using Advanced Research Weather Research and Forecasting Model. *Nat. Hazards*, **73**, 1043-1062.
- Tao, W., J. J. Shi, S. S. Chen, S. Lang, P. Lin, S.-Y. Hong, C. P. Lidard, and A. Hou, 2011: Impact of microphysical schemes on hurricane intensity and track. *Asia-Pac. J. Atmos. Sci.*, **47**, 1-16.
- Trivedi, D. K., J. Sanjay, and S. S. Singh, 2002: Numerical simulation of a super cyclonic storm, Orissa 1999: Impact of initial conditions. *Meteor. Appl.*, **9**, 367-376.
- _____, P. Mukhopadhyay, and S. S. Vaidya, 2006: Impact of physical parameterization schemes on the numerical simulation of Orissa super cyclone (1999). *Mausam*, **57**, 97-110.
- Tuleya, R. E., and Y. Kurihara, 1981: A numerical study on the effects of environmental flow on tropical storm genesis. *Mon. Weather Rev.*, **109**, 2487-2506.
- Wang, Y., and C.-C. Wu, 2004: Current understanding of tropical cyclone structure and intensity changes - A review. *Meteor. Atmos. Phys.*, **87**, 257-278.
- White, B., J. Paegle, W. J. Steenburgh, J. D. Horel, R. T. Swanson, L.K. Cook, D. J. Onton, and J. G. Miles, 1999: Short-term forecast validation of six models. *Wea. Forecasting*, **14**, 84-108.
- Wu, C.-C., and H.-J. Cheng, 1999: An observational study of environmental influences on the intensity changes of Typhoons Flo (1990) and Gene (1990). *Mon. Wea. Rev.*, **127**, 3003-3031.
- Yesubabu, V., C. V. Srinivas, S. S. V. S. Ramakrishna, and K. B. R. R. Hariprasad, 2014: Impact of period and timescale of FDDA analysis nudging on the numerical simulation of tropical cyclones in the Bay of Bengal. *Nat. Hazards*, **74**, 2109-2128.
- Zehr, R. M., 1992: Tropical cyclogenesis in the western North Pacific. NOAA Tech. Rep. NESDIS 61, 181.
- Zeng, Z., Y. Wang, and C. C. Wu, 2007: Environmental dynamical control of tropical cyclone intensity - An observational study. *Mon. Wea. Rev.*, **135**, 38-59.